15 Noble Gases in Ocean Waters and Sediments

Peter Schlosser[1,2] and Gisela Winckler[1]

Lamont-Doherty Earth Observatory
Columbia University
Palisades, New York 10964

[2] *Department of Earth and Environmental Sciences*
and *Department of Earth and Environmental Engineering*
Columbia University
New York, New York 10027
peters@ldeo.columbia.edu

INTRODUCTION

Noble gases are widely used in studies of the basic properties and dynamics of natural systems including the ocean. This chapter describes some of the more extensive applications of noble gases (mainly helium isotopes) to studies of oceanographic problems. They include the modern oceanic circulation, paleo-oceanography, hydrothermal and cold brine systems in the deep ocean, and ocean/atmosphere gas exchange.

Originally, oceanic noble gas studies were focused on geochemical problems such as the question of the existence of excess helium in seawater derived from radioactive decay of the elements of the uranium and thorium series in ocean sediments (Suess and Wänke 1965; Bieri et al. 1966). After the discovery of mantle (primordial) helium during the 1960s (Clarke et al. 1969; Craig and Weiss 1971; Craig et al. 1975) and ^{3}He derived from decay of tritium in the near-surface waters of the ocean (Jenkins and Clarke 1976), large programs were developed to exploit helium isotopes, frequently in combination with tritium, for studies of water mass formation, circulation and variability (e.g., Jenkins 1987; Schlosser et al. 1991).

More recent studies started to explore the use of helium isotopes to paleoceanographic objectives. These studies build upon the discovery of extraterrestrial helium in deep-sea sediments in the early 1960s (Merrihue 1964). This signal is now being systematically examined for its potential as a tool for investigations of sediment accumulation rates on very long time scales (millions of years) and their correlation with changes in paleoceanography (e.g., Farley 1995; Farley and Patterson 1995; Marcantonio et al. 1995, 1996, 2001).

Soon after the discovery of mantle helium in seawater, noble gases were applied to studies of hydrothermal systems. Originally, these studies were focused on the source of the fluids emanating from hydrothermal vents as well as the related heat flux. More recent studies use the full set of noble gases to infer processes of the formation and dynamics of hydrothermal systems at the sea floor.

Field studies of ocean/atmosphere gas exchange originally were concentrated around naturally existing isotopes such as ^{222}Rn and ^{14}C (Roether and Kromer 1978; Broecker and Peng 1982; Smethie et al. 1985). Later studies included so-called 'bomb' ^{14}C. However, since gas exchange rates derived from these methods had considerable uncertainties, new methodologies were explored. One of them includes the injection of two gas tracers with similar solubility and strong differences in their diffusion constants (e.g., Watson et al. 1991; Wanninkhof et al. 1993, Nightingale et al. 2000a,b). The most promising dual tracer pair is the combination of ^{3}He and SF_6.

The following paragraphs outline the basic methodologies behind the use of helium

1529-6466/02/0047-0015$05.00 DOI:10.2138/rmg.2002.47.15

isotopes and the heavier noble gases in the areas described above. Instead of presenting a comprehensive review of all studies that were performed in the individual fields, we focus on the basic principles and use exemplary studies to demonstrate applications and results.

TRACING OCEAN CIRCULATION USING ^{3}HE AND TRITIUM

^{3}He can be used in studies of the oceanic circulation in two ways: (1) through the simultaneous measurement of ^{3}He and its radioactive parent isotope tritium, and (2) by mapping the plumes of mantle helium injected into the intermediate depth waters of the world oceans.

Tritium/^{3}He method

Tritium geochemistry. Tritium is the radioactive isotope of hydrogen that decays by β-decay to the noble gas ^{3}He ($t_{1/2}$ = 12.43 yr; Unterweger et al. 1980; note that Kipfer et al. use a slightly different half-life in the previous chapter). Natural tritium is produced by interaction of cosmic rays with nitrogen and oxygen mainly in the upper atmosphere. After oxidation to HTO, tritium takes part in the hydrological cycle. The potential of tritium for applications to studies of the natural water cycle has been realized shortly after its detection in the environment (von Faltings and Harteck 1950; Grosse et al. 1951; Kaufman and Libby 1954; Begemann and Libby 1957; Giletti et al. 1958).

Natural tritium concentrations in ocean surface waters and in young groundwater are of the order of 1 tritium atom per 10^{18} hydrogen atoms. This is the reason that tritium concentrations are reported as TU (Tritium Units). One TU stands for a tritium to hydrogen ratio [^{3}H]/[H] of 10^{-18}. The activity of a water sample with a tritium concentration of 1 TU is equivalent to 3.2 pCi or 0.12 Bq per liter of H_2O. The production rate of natural tritium is about 0.5±0.3 ^{3}H atoms cm^{-2} s^{-1} (Craig and Lal 1961) leading to natural tritium values in ocean surface waters of about 0.2 TU (Dreisigacker and Roether 1978).

Before natural tritium could be fully exploited for studies of natural water systems, tritium from anthropogenic sources (mainly nuclear weapon tests) was added to the atmosphere in considerable amounts. By the mid 1960s the natural background of tritium in precipitation was practically masked by so-called bomb tritium (e.g., Weiss et al. 1979; Fig. 1). For the past 4 to 5 decades, bomb tritium severely limited the use of natural tritium as a tracer because only few uncontaminated tritium data are available from the pre-bomb era. However, bomb tritium offered a new tool for studies of water movement in natural system. It is equivalent to a ‘dye’ that was introduced into the environment on a global scale at a relatively well-known rate. Most of the bomb tritium was added to the environment in three pulses during 1954, 1958-1959 and, predominantly, 1963.

During the following three decades the application of bomb tritium has been developed to a routine tool in studies of natural water systems (e.g., Münnich and Roether 1967; Roether et al. 1970; Atakan et al. 1974; Östlund 1982; Broecker et al. 1986).

The surface waters of the ocean are the largest sink for tritium. Transfer into the surface ocean occurs by water vapor exchange, precipitation and continental run-off (e.g., Weiss et al. 1979; Weiss and Roether 1980). Most of the nuclear weapons tests were performed in the northern hemisphere, leading to a strong asymmetry in the global north-south distribution of bomb tritium in the ocean surface waters. Concentrations in the northern hemisphere are relatively high compared to those in the southern hemisphere (Weiss and Roether 1980; Fig. 1).

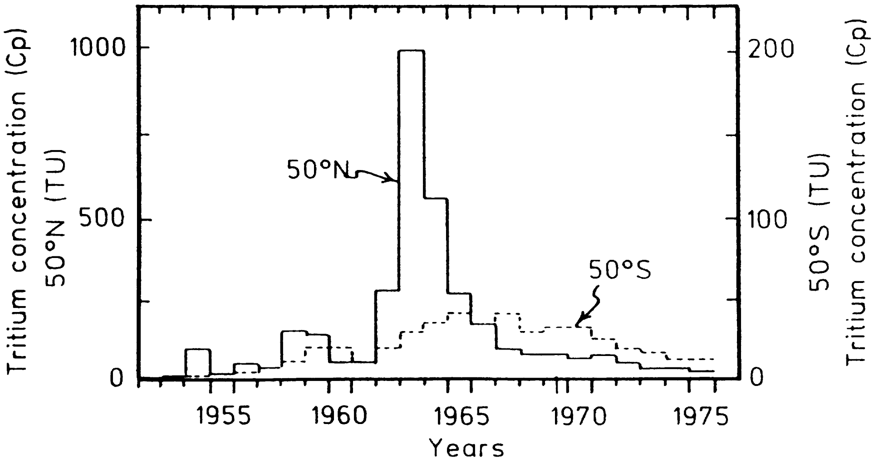

Figure 1. Tritium concentration in marine precipitation at 50°S and 50°N as a function of time (after Weiss and Roether 1980). Note the different scales for the tritium concentrations in the Northern and Southern hemisphere.

Presently, maximum tritium concentrations in the surface waters of the oceans are approximately 1.5 to 2 TU in the northern hemisphere and 0.20 to 0.75 TU in the southern hemisphere. Regions that receive high concentrations of runoff such as the Arctic Ocean or locations surrounded by continents such the Mediterranean and Red seas exhibit elevated tritium concentrations.

Tritiogenic ^{3}He and tritium/^{3}He age. Limitations in using tritium alone as oceanographic tracer arise from the shape of its 'input function', i.e., the evolution of the transfer rate of tritium to the surface waters of the ocean (Fig. 1). The gradient in the surface waters decreased significantly during the 1970s and 1980s, and presently it is too small to be of much use for determination of relative age fields. Additionally, it is difficult to detect the bomb peak in the interior of the ocean, typically preventing the use of tritium as an absolute age marker.

Simultaneous measurement of tritium and its radioactive decay product, ^{3}He, helps to at least partially eliminate these problems. Combined measurement of tritium and ^{3}He allows us to calculate the tritium/^{3}He age. This tracer age is a measure for the time that elapsed since a water parcel has been isolated from exchange with the atmosphere. During this process tritium is taken up and ^{3}He is lost to the atmosphere by gas exchange, i.e., the 'tritium/^{3}He 'clock' is set to zero. Jenkins and Clarke (1976) introduced this method to oceanography. The tritium/^{3}He age is calculated as follows (see also Kipfer et al. 2002, this volume):

$$\tau = \frac{T_{1/2}}{\ln 2} \cdot \ln\left(1 + \frac{[^3\mathrm{He}_{\mathrm{tri}}]}{[^3\mathrm{H}]}\right) \tag{1}$$

where $T_{1/2}$ is the half-life of tritium, [^{3}He$_{\mathrm{trit}}$] the tritiogenic ^{3}He concentration of the water sample, and [^{3}H] the tritium concentration of the water at the time of sample collection. Solution of this equation requires the calculation of the tritiogenic ^{3}He concentration, i.e., the fraction of the measured ^{3}He concentration that has been added to the water by radioactive decay of tritium.

Helium observed in natural water samples has several sources that may be distinguished by their ^{3}He/^{4}He ratio. Generally, atmospheric helium with a ^{3}He/^{4}He ratio of 1.384×10^{-6} (Clarke et al. 1976) is the major component present in natural waters. Its solubility is a function of the temperature and salinity of the water (Weiss 1971). ^{3}He is slightly less soluble in water than ^{4}He, leading to a small ^{4}He-enrichment in water which is in solubility equilibrium with the atmosphere (solubility isotopic fractionation $\alpha \approx 0.983$, Benson and Krause 1980). Usually excess of atmospheric helium above the thermodynamic solubility equilibrium is observed. In the case of open water reservoirs, this excess is caused by interaction of the surface water with small air bubbles introduced into the surface layer by breaking waves (gas exchange and dissolution). However, in the vicinity of glacial ice sheets (e.g., around Antarctica), melting of glacial ice at depth can produce significant helium and neon excesses due to dissolution of air trapped during transition from firn to ice. This signal can be used to trace water masses formed in contact with glacial ice from the shelves into the deep sea (for details of the method and applications to oceanography, see, e.g., Schlosser 1986; Schlosser et al. 1990; Weppernig et al. 1996; Hohmann et al. 2002). Besides the atmospheric helium, a water sample may contain mantle-derived helium characterized by high ^{3}He/^{4}He ratios (of the order of 10^{-5}, Craig and Lupton 1981). Finally, natural water samples may contain radiogenic helium with low ^{3}He/^{4}He ratios (of the order of 10^{-7} to 10^{-8}; characteristic value: 2×10^{-8}, Mamyrin and Tolstikhin 1984). Radiogenic helium is produced by the α-decay of the natural radioactive decay series and contains a ^{3}He component originating mainly from the ^{6}Li(n,α)^{3}H reaction. The ^{3}He balance, including tritiogenic ^{3}He, is given in Equation (2):

$$^3\mathrm{He}_\mathrm{m} = {}^3\mathrm{He}_\mathrm{eq} + {}^3\mathrm{He}_\mathrm{ex} + {}^3\mathrm{He}_\mathrm{ter} + {}^3\mathrm{He}_\mathrm{tri} \tag{2}$$

with: $^3\mathrm{He}_\mathrm{m}$ = measured ^{3}He concentration of the water sample, $^3\mathrm{He}_\mathrm{tri}$ = tritiogenic ^{3}He, $^3\mathrm{He}_\mathrm{eq}$ = ^{3}He concentration in solubility equilibrium with the atmosphere, $^3\mathrm{He}_\mathrm{ex}$ = ^{3}He originating from excess air, and $^3\mathrm{He}_\mathrm{ter}$ = terrigenic ^{3}He (crustal and mantle helium).

To separate tritiogenic ^{3}He from the total ^{3}He of the water sample (Eqn.3), both ^{4}He and neon are used as indicators of atmospheric and terrigenic helium.

$$^3\mathrm{He}_\mathrm{tri} = {}^4\mathrm{He}_\mathrm{m} \cdot \mathrm{R}_\mathrm{m} - \left({}^4\mathrm{He}_\mathrm{m} - {}^4\mathrm{He}_\mathrm{ter}\right) \cdot \mathrm{R}_\mathrm{a} + {}^4\mathrm{He}_\mathrm{eq} \cdot \mathrm{R}_\mathrm{a} \cdot (1-\alpha) - {}^4\mathrm{He}_\mathrm{ter} \cdot \mathrm{R}_\mathrm{ter} \tag{3}$$

where R_m and $^4\mathrm{He}_\mathrm{m}$ are the measured ^{3}He/^{4}He ratio and ^{4}He concentration of the water sample, respectively, R_ter and $^4\mathrm{He}_\mathrm{ter}$ are the ^{3}He/^{4}He ratio and ^{4}He concentration of the terrigenic helium component, respectively, and R_a is the ^{3}He/^{4}He ratio of atmospheric helium. If both mantle helium and radiogenic helium are present in a water sample in addition to atmospheric helium, the individual helium components cannot be separated in a straightforward way. If only mantle helium or radiogenic helium is contained in the water, it is easier to separate the tritiogenic ^{3}He because in this case reasonable estimates for the ^{3}He/^{4}He ratios of the added helium components are available. In the Pacific and Indian oceans, the mixing of mantle helium from intermediate waters with low tritium concentrations into the near-surface waters for which most of the oceanic tritium/^{3}He age dates are calculated, complicates tritium/^{3}He dating. In this case ^{3}He/silica correlations can be used to separate the mantle-derived ^{3}He from the tritiogenic ^{3}He (see Jenkins 1996).

Details on the separation of $^3\mathrm{He}_\mathrm{tri}$ are given by Schlosser (1992) and Well et al. (2001), among others. In most ocean environments, the contribution of the radiogenic ^{4}He signal is small and typically can be neglected.

^{3}He results of oceanographic water samples are usually reported in the δ notation where δ^3He means the percent deviation of the measured ^{3}He/^{4}He ratio of a water sample (R_m) from that of an air standard (R_a)

$$\delta^3\mathrm{He} = \left(\frac{\mathrm{R}_\mathrm{m}}{\mathrm{R}_\mathrm{a}} - 1\right) \cdot 100\% \tag{4}$$

In many cases it is more convenient to use the TU notation for ^{3}He concentrations. ^{3}He concentrations in TU are obtained from Equation (5):

$$^3\mathrm{He}_{\mathrm{trit}} = 4.021\times10^{14}\left[\frac{^4\mathrm{He}_\mathrm{m}\cdot\left(\mathrm{R}_\mathrm{m}-\mathrm{R}_\mathrm{a}\right)+{}^4\mathrm{He}_\mathrm{eq}\cdot\mathrm{R}_\mathrm{a}\cdot(1-\alpha)}{\frac{1-\mathrm{S}}{1000}}\right] \tag{5}$$

where S is the salinity of the water sample in psu. If all the tritium of a water sample (S = 0) with a tritium concentration of 1 TU decays, it results in a tritiogenic ^{3}He concentration of 2.49×10^{-15} cm^3 STP. This leads to an increase in δ^3He of about 3.86% based on a salinity of 0 and a temperature of 9°C (^{4}He solubility equilibrium concentration: 4.66×10^{-8} cm^3 g^{-1}; Weiss 1971).

The tritium/^{3}He age does not depend on the initial tritium concentration of the water parcel. This means that the initial tritium concentration of a water parcel that is determined by the tritium delivery does not have to be known for calculating a tracer age. Typically, the delivery rate of tritium to natural water bodies is not known exactly and in certain regions estimates of the delivery rate can be very difficult and inaccurate. The tritium/^{3}He age is an apparent age and can only be taken as the true age of the water if ^{3}He sources other than tritium decay (^{3}He derived from mantle helium or nucleogenic ^{3}He found in radiogenic helium) can be excluded or corrected for, and mixing with water of different tritium and ^{3}He concentrations is negligible or can be quantified. The tritium/^{3}He age is non-linear with respect to mixing (Jenkins and Clarke 1976). For illustration of this problem, two mixing lines are drawn in a plot of the isochrones calculated from Equation (10) (A-B and A′-B′ in Fig. 2). In both cases the tritium/^{3}He age of the mixture is weighted in favor of the water with the higher tritium concentration (Fig. 2). The logarithmic function of the tritium/^{3}He age causes non-linearities even in cases of equal tritium concentrations. If water with no tritium and no ^{3}He is added to a certain water parcel, its tritium/^{3}He age is not affected, since the mixing is along the isochrones.

The age resolution of the tritium/^{3}He method is determined mainly by the measurement precision of the ^{3}He/^{4}He ratio (e.g., Schlosser 1992). On the basis of a

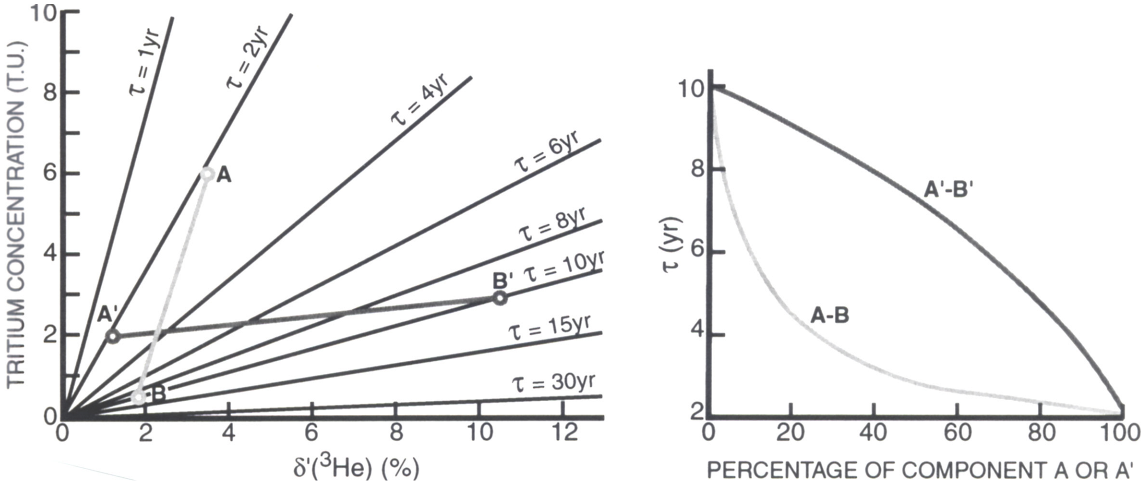

Figure 2. Tritium/^{3}He isochrones in years (left) and non-linearity of the tritium/^{3}He age with respect to mixing along the lines A-B and A'-B' (right), after Jenkins (1974). In both cases, the tritium/^{3}He age of the mixture is weighted in favor of the water mass with the higher tritium concentration.

^{3}He/^{4}He precision of ±0.2%, the age resolution is calculated and plotted in Figure 3. For waters with tritium concentrations of about 50 TU (shallow groundwater) an age resolution of about one week can be achieved. For northern hemisphere ocean surface waters with tritium concentrations of about 2 TU the time resolution is of the order of 6 to 12 months, and for Southern Hemisphere surface waters (≈ 0.5 TU) the time resolution is no better than about 3 years if it is possible to separate the tritiogenic ^{3}He from the total ^{3}He measured in the water. The age resolution given here is that of the apparent tritium/^{3}He age and does not take into account systematic errors such as mixing.

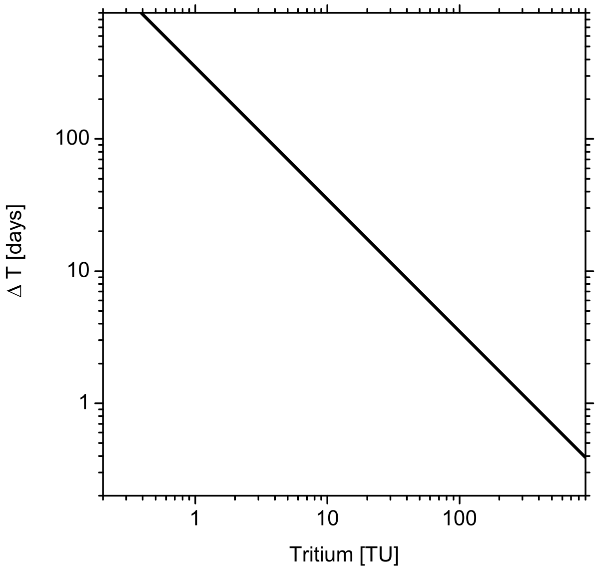

Figure 3. Time-resolution of the tritium/^{3}He method as a function of the tritium concentration of a water sample calculated on the basis of a measurement precision of ±0.2% for δ^3He. After Schlosser (1992).

Exemplary results from tritium/^{3}He studies

Applications of the tritium/^{3}He method to problems of the oceanic circulation started in the early 1970s when, as part of the GEOSECS (Geochemical Ocean Sections) program, Jenkins and Clarke (1976) conducted a systematic study of the distribution of these isotopes in the Atlantic Ocean. This study was followed by numerous tritium/^{3}He programs that addressed ocean circulation or oxygen utilization on regional and/or global scales (e.g., Thiele et al. 1986; Jenkins 1987; Roether and Fuchs 1988; Doney and Jenkins 1994; Schlosser et al. 1995; Bönisch et al. 1997; Jenkins 1998; Robbins et al. 2000, to name just a few).

The penetration of tritium into the interior of the ocean can be followed through repeated observations over a certain period of time. Such observations reveal pathways of water masses, as well as insight into the general penetration patterns of perturbations imprinted onto the surface of the ocean. In the interior of the ocean, tritium decay leads to a buildup of tritiogenic ^{3}He and tritium/^{3}He ages can be calculated. Evaluation of the tritium/^{3}He age distributions, especially if performed in conjunction with model simulations that correct for the non-linearities of the apparent tritium/^{3}He age, provides valuable information on mean spreading rates of water masses (e.g., Doney and Jenkins 1994), average mixing coefficients (e.g., Thiele et al. 1986), variability of water masses (e.g., Schlosser et al. 1991), as well as geochemical rates such as oxygen utilization rates (e.g., Jenkins 1982, 1987).

Instead of attempting a comprehensive review of the oceanic tritium/^{3}He literature, we present examples of two types of applications: dye-type penetration of tritium into the surface layers of the ocean and variability in deep water formation rates.

Ventilation of the oceanic thermocline. The spatial resolution of the WOCE (World

Ocean Circulation Experiment) tritium/helium isotope survey exceeds that achieved during the GEOSECS program by a factor of ~10. The data density obtained from this survey is sufficiently high to allow 3-dimensional visualizations of the tritium plumes in the ocean. In this way, the WOCE tritium/^{3}He sections (for an example, see Fig. 4)

(a) Tritium

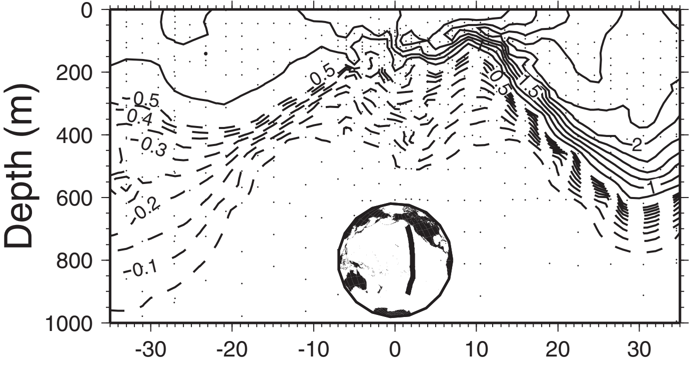

(b) Excess ^{3}He

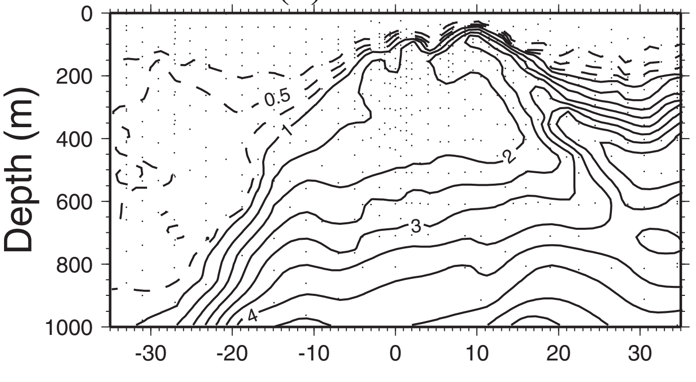

(c) ^{3}H-^{3}He Age

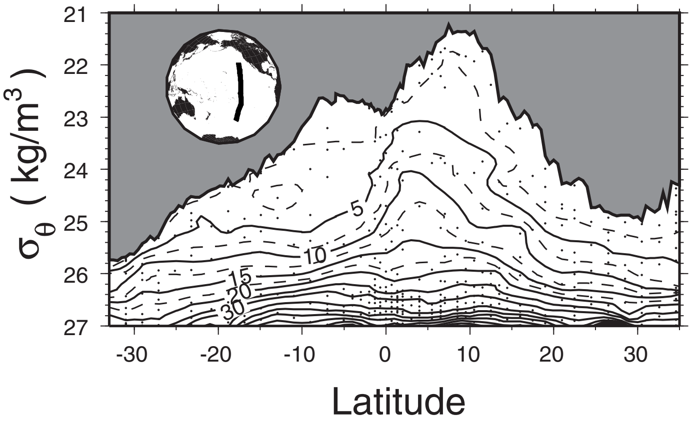

Figure 4. Distribution of tritium (a), ^{3}He (b), and tritium/^{3}He age (c) along 135ºW (WOCE section P17C) occupied in 1991. The data delineate the penetration pattern of bomb tritium from the surface into the interior of the Pacific Ocean. The apparent tritium/^{3}He ages can be used to derive information on the mean residence times of the waters in the thermocline of the Pacific Ocean. After Schlosser et al. (2001).

provide valuable information on the spreading of water masses from the surface into the interior of the ocean (e.g., Jenkins 1998). If we combine the tritium and the tritiogenic ^{3}He distributions, we can derive information on mean residence times ('ages') of specific water masses (Fig. 4c). These apparent ages provide a good measure for the time it takes a water mass to spread from the surface where it equilibrates with the atmosphere to the point of interest in the interior of the ocean. For example, the spreading of water masses from the subtropical gyre in the Pacific to the equator takes of the order of a few years to a decade depending on the depth of the water mass (Fig. 4c).

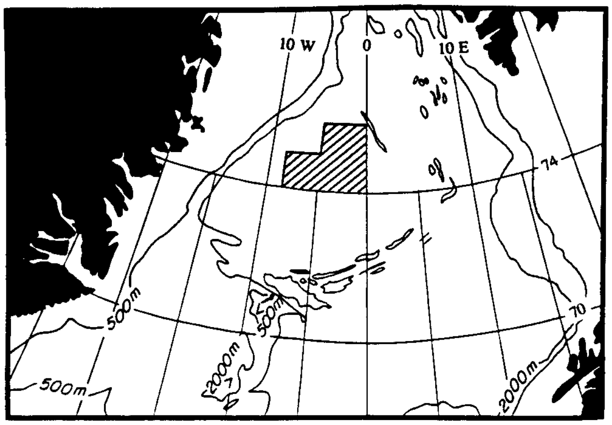

Figure 5 (left). Geographical location of the Greenland time-series experiment. From Bönisch et al. (1997).

Figure 6 (below). Time series of the tritium concentration (left panel), δ^3He (middle), and tritium/^{3}He age (right) in the Central Greenland Sea. The declining tritium concentrations in the waters below ~2000-m depth, together with the quasi-linear increase in the tritium/^{3}He can be used to derive the reduction in Greenland Sea Deep Water formation. For detailed explanation, see text. After Bönisch et al. (1997).

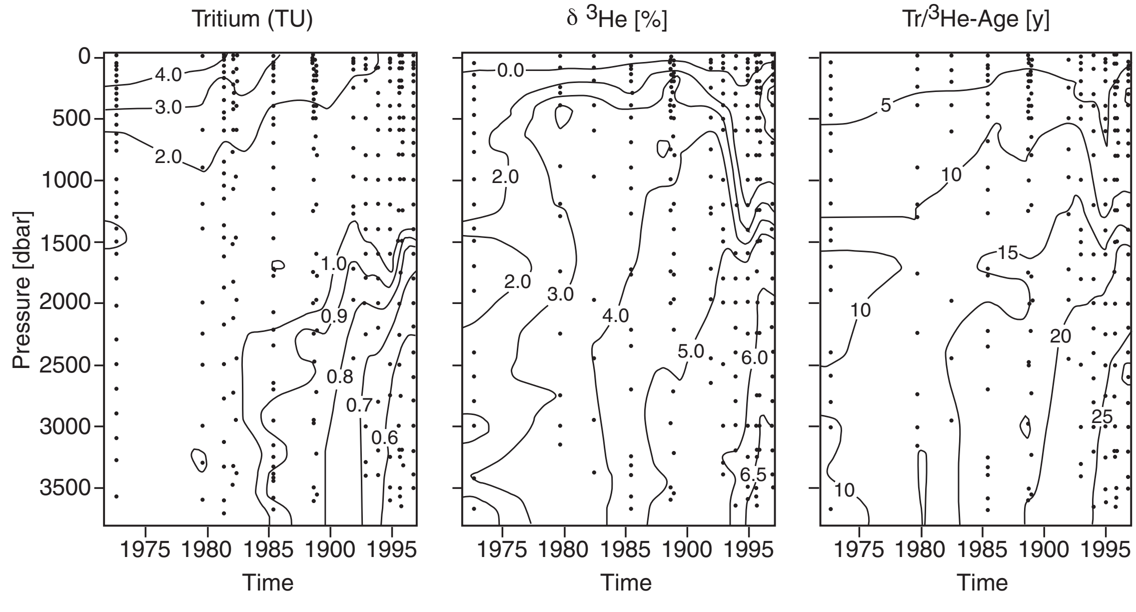

Studies of variability of water mass renewal in the ocean. Time series of tritium and ^{3}He have been used to study the temporal evolution of water mass characteristics in certain regions of the ocean, including the Sargasso Sea (Robbins and Jenkins 1998) and the Greenland Sea (Schlosser et al. 1991; Bönisch et al. 1997). Such time series, especially if combined with model simulations of the region reveal average water mass formation rates, as well as their variability. The Greenland Sea time series (Fig. 6; for geographical position of the stations, see Fig. 5) indicates a steady decrease of tritium throughout the water column, whereas the concentrations of ^{3}He and the tritium/^{3}He age are increasing in the deep water. The decreasing near-surface tritium concentrations reflect the decrease in the tritium delivery from the atmosphere to the surface ocean. The increase in ^{3}He and the tritium/^{3}He age in the deep water (depths below 1500 m), on the other hand, are evidence for a change in the formation rate of deep water in the Greenland Sea at around 1980. The tritium/^{3}He data, together with CFC data and a simple time-dependent mass balance (box model) were used to quantify the reduction in the rate of deep-water formation that occurred at this time in the center of the Greenland Sea. The reduction rate was estimated to be about 80% (from 0.5 Sv to 0.1 Sv, Schlosser et al. 1991; Bönisch and Schlosser 1995; 1 Sv = 10^6 m^3 sec^{-1}). Without tracer data the reduction in deep water renewal could not have been quantified with the same accuracy.

This change is significant and persisted between 1980 and 2000, the time of the last tracer observations in the central Greenland Sea. It led to a significant change in the characteristics of the deep waters in the Greenland Sea. For example, the temperature and salinity properties of Greenland Sea Deep Water observed in the mid- and late 1990s fall outside the classical definitions of this water mass (Bönisch et al. 1997). The deep water that in the past was formed by deep convection from the surface is slowly replaced by warmer and saltier waters originating in the Arctic Ocean and the Norwegian Sea. Whereas we were able to document the change in deep water formation in the central Greenland Sea by measuring a variety of variables and to quantify its reduction using transient tracers including tritium/^{3}He, we do not yet have a solid explanation for the cause of the reduction in deep water formation. The high northern latitude oceans, especially the Arctic Ocean, are presently undergoing significant changes (e.g., Morison et al. 1998, 2000). There is a distinct possibility that part of these changes are going beyond the natural variability and represent early signs of anthropogenically induced trends.

MANTLE ^{3}HE

General background

Although the early search for helium in the oceans was driven by the hypothesis that the ocean should show a signature of excess ^{4}He derived from α -decay of elements of the uranium and thorium decay series in the sediments (Suess and Wänke 1965), the attention turned to mantle-derived ^{3}He as soon as the first helium isotope profiles had been measured in the mid/late 1960s in the South Pacific and as part of the preparations for the GEOSECS program in the North Pacific (Clarke et al. 1969; Clarke et al. 1970). These measurements revealed elevated ^{3}He/^{4}He ratios in the deep waters of the Pacific Ocean (up to several ten percent). The excess ^{3}He estimated from the helium isotope measurements were attributed to so-called primordial helium, i.e., helium that was trapped in the interior of the Earth during its formation (Clarke et al. 1969). Measurements of helium isotopes in thermal fluids (Mamyrin et al. 1969) and deep sea basalts confirmed this hypothesis and the ^{3}He/^{4}He ratio of the mantle-derived helium was determined to be approximately 8 times that of the atmosphere, i.e., roughly 1×10^{-5} (Krylov et al. 1974; Lupton and Craig 1975). These findings provided unambiguous evidence not only that the earth contains a primordial volatile component from its accretion but also that degassing of primordial volatiles is still occurring at mid-ocean ridges and hot spots.

Geochemical background

Hydrothermal activity is a common phenomenon found in the deep sea on a global scale, mainly along the mid-ocean ridges. Hydrothermal vents discharge fluids that contain a variety of trace elements, including noble gases. Helium emanated by deep-sea hydrothermal vents is strongly enriched in the light isotope ^{3}He. Frequently, helium isotope ratios in fluids from deep-sea hydrothermal vents are close to those of Mid Ocean Ridge Basalt (MORB, R/R_a = 8-9, Craig and Lupton 1981). However, due to the large variation in helium isotope ratios in fluids emanating from all possible deep-sea sources, including seamounts, the range of observed helium isotope ratios is large (ca. 3 to 30 times the atmospheric ratio). Such a variety in helium isotope ratios can be used to track different sources of helium observed in the intermediate waters of the ocean (Lupton 1996, 1998; see below). Along with the elevated helium isotope ratios, the absolute ^{3}He concentrations in hydrothermal fluids (ca. 0.2 to 2.5×10^{-9} cm^3 STP g^{-1}) are elevated by several orders of magnitude above background ^{3}He concentrations in water that has been equilibrated with the atmosphere (ca. 6×10^{-14} cm^3 STP g^{-1}, e.g., Butterfield et al. 1990). Helium injected in the deep sea follows the circulation of the water masses to which it is added. Eventually, it is released from the ocean to the atmosphere by air/sea gas exchange. Due to different source strength (spreading rates of the mid-ocean ridges; Lupton 1998) and mean residence times in the major ocean basins, the mean ^{3}He excess related to injection of mantle helium into the intermediate depth waters of the ocean differs from basin to basin. The highest values are found in the Pacific (ca. 20%; Lupton 1998), the lowest in the Atlantic (1 to 2%; e.g., Rüth et al. 2000). The Indian Ocean excess has been estimated on the basis of model simulations to be about 10% (Farley et al. 1995; see also Östlund et al. 1987 for data tables and sections).

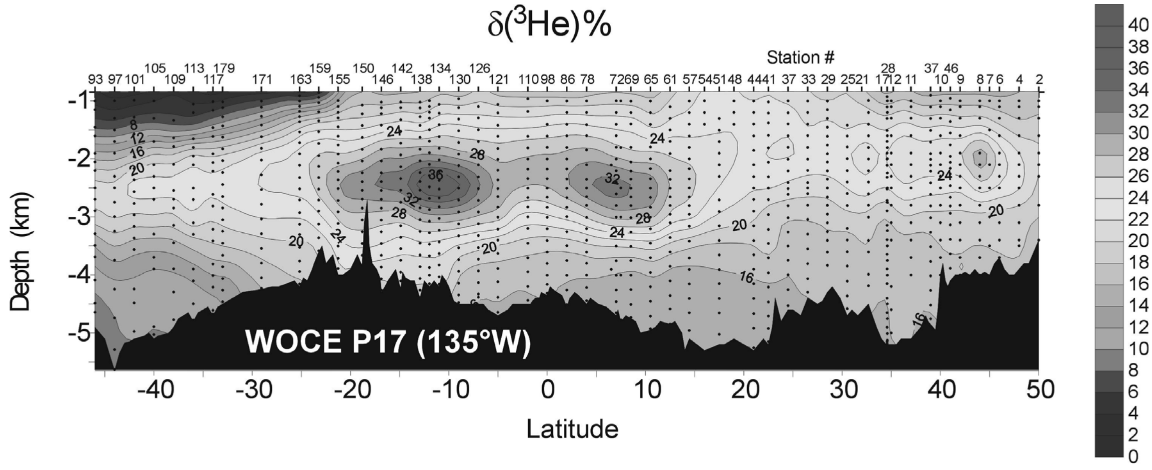

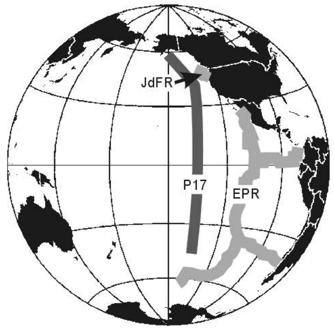

Figure 7. δ^{3}He distribution along 135ºW (WOCE section P17C) from 1000-m depth to the bottom (contour interval is 2%). From Lupton (1998).

^{3}He plumes in the ocean

After initial systematic surveys could be completed during the 1970s, it became apparent that the ^{3}He emanating from the mid ocean ridges formed large-scale plumes (e.g., Lupton et al. 1980; Lupton and Craig 1981) that can be used to study the oceanic circulation on mid-depth strata. Further investigations during the past two decades, including sections from the World Ocean Circulation Experiment, led to systematic mapping of large-scale ^{3}He plumes in the major ocean basins. This work has been progressed the farthest for the Pacific Ocean (Lupton 1996, 1998; Schlosser et al. 2001).

In addition to the large plume emanating from the East Pacific Rise at 10°N and 15°S (EPR, Lupton et al. 1980) discovered early on, at least two other major ^{3}He sources have been detected and described in the Pacific Ocean, e.g., Lupton, 1996, 1998). One is emanating from the Juan de Fuca Ridge in the northeastern Pacific at 48°N and one from Loihi Seamount near Hawaii at 20°N. All three plumes can be recognized in a N/S section across the central Pacific at about 135W (WOCE line P17, Fig. 7) and can be separated by depth (Lupton 1998). The EPR plume is situated deep in the water column (~2500 m). The Juan de Fuca Ridge plume is found somewhat higher in the water column (~2000-m depth) and the Loihi seamount plume is rather shallow (~1100 m). The Loihi plume is different from the others in that it is fed from a hot spot source and not from mid-ocean ridge vents. The spreading pattern of the plumes can be derived from horizontal ^{3}He maps in the Pacific as demonstrated by Lupton (1996, 1998). Whereas the EPR and Juan de Fuca Ridge plumes indicate westward spreading (the EPR plume spreads across the entire Pacific Basin), the Loihi seamount plume has an eastward movement (Fig. 8). Work similar to that in the Pacific Ocean was performed in the South Atlantic by Rüth et al. (2000). Here, the mantle ^{3}He signals are much smaller due to the slower spreading rates of the mid ocean ridge and the ^{3}He signatures and patterns are more difficult to translate into information on the oceanic circulation. The Indian Ocean ^{3}He data from WOCE are presently being evaluated and first unpublished results look very promising, indicating ^{3}He plumes from at least three different sources (mid ocean ridge, Indonesian Throughflow, and Gulf of Aden).

Most of the evaluation of the ^{3}He plumes in the ocean has been qualitative or semi-quantitative in nature. However, there are increasing attempts to incorporate ^{3}He into Ocean General Circulation Models (OGCMs) in order to understand how such models ventilate the mid-depth and deep-water masses. An early attempt of ^{3}He simulations in an OGCM has been documented by Farley et al. (1995). The results of the model simulations indicate that the model can roughly close the helium balance and reproduces most of the major observed features of the ^{3}He field in the ocean. At the same time, the simulations show many shortcomings of the model and future work will contribute to both a better understanding of the ^{3}He plumes and the quality of ocean circulation models.

THE FLUX OF ^{3}HE AND ^{4}HE FROM THE SEAFLOOR

^{4}He

On the basis of mass balance considerations, Suess and Wänke (1965) postulated that the flux of ^{4}He produced by U and Th decay in the deep-sea sediments should be detectable as a ^{4}He excess in the abyssal waters of the ocean. Early measurements of helium dissolved in seawater were difficult and interpretation of the results was challenging. For example König et al. (1964) interpreted their results as consistent with solubility data, whereas Suess and Wänke (1965) used the same measurements to support their hypothesis that there should be a measurable helium excess related to a sediment source. Bieri et al. (1966) reported noble gas measurements from Pacific waters and concluded that there has to be a terrestrial helium source at the sediment interface that supplies the excess helium observed in the water column. Whereas these early studies focused on radiogenic helium as the source of the observed excess helium, the introduction of helium isotope measurements revealed that there are two sources of terrigenic helium that contribute to the observed helium excess. In addition to the crustal (radiogenic) ^{4}He there is a contribution of mantle-derived helium that is enriched in ^{3}He by roughly a factor of 8. The presence of helium from two terrigenic sources and the added complication of a helium excess due to the (partial) dissolution of air at the sea surface and close to floating ice shelves (e.g., Schlosser 1986; Schlosser et al. 1990)

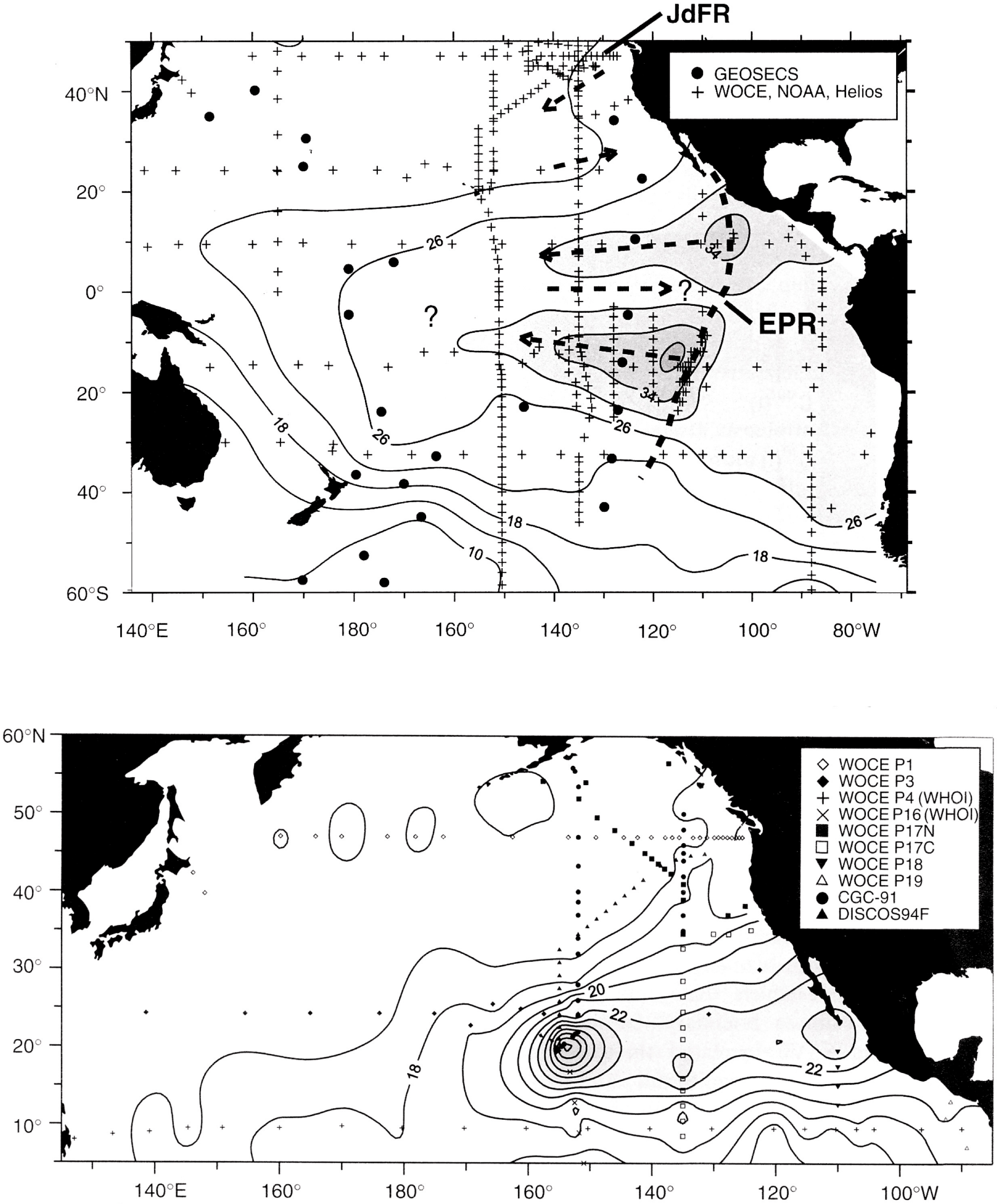

Figure 8. Map of δ^3He (%) contoured on a surface at 2500 m depth (upper panel, contour interval is 4%) and on a surface of 1100 m depth (lower panel, contour interval is 1%) in the Pacific Ocean. Large ^{3}He-rich plumes emanate from the East Pacific Rise (EPR) at 15°S and 10°N and Juan de Fuca Ridge (JdFR) systems and spread westward, as indicated by the dashed arrows. Question marks denote regions where flow patterns are not obvious from the δ^3He distribution. The helium signal emanating from Loihi Seamount, on the southeastern flank of Hawaii, is transported eastward as a continuous plume to the coast of Mexico. Plot produced by John Lupton using data from Lupton (1998) and unpublished data produced by W. J. Jenkins. [Used by permission of Academic Press, from Schlosser et al. (2001), *International Geophysics Series*, Vol. 77, Fig. 5.8.14 and 5.8.16, p. 442 and 443]

makes it fairly difficult to accurately quantify the ^{4}He flux from the sea floor. In typical oceanographic water masses, ^{4}He from the individual helium sources is difficult to separate and the amounts of excess ^{4}He in typical water samples is relatively small if compared to the ^{3}He excesses related to the addition of mantle helium.

Based on the observed ^{4}He excess and turnover time of the Pacific Ocean Craig et al. (1975) estimated the oceanic ^{4}He flux to be $3\pm1\times10^5$ atoms cm^{-2} s^{-1} if referred to the area of the entire oceanic crust. This estimate includes both the hydrothermal ^{4}He flux emanating from mid-ocean ridges as well as the crustal ^{4}He flux by degassing of the oceanic crust. The oceanic ^{4}He flux is small compared to the total ^{4}He flux of ca. 1.3×10^6 atoms cm^{-2} s^{-1} (normalized to the entire earth surface).

There are specific regions in the ocean where strong ^{4}He signals can be observed. For example, ^{4}He excesses in the Black Sea (Top and Clarke 1983) and the Eastern Mediterranean (Roether et al. 1998) were converted into ^{4}He fluxes and yielded values of $1.3\pm0.5\times10^6$ and $3.1\pm1.2\times10^6$ atoms cm^{-2} s^{-1}, respectively. These values are comparable to the fluxes estimated for the continental crust ($2.7\pm1\times10^6$ atoms cm^{-2} s^{-1} normalized to the continental area; e.g., Torgersen 1989). This shows that on a local/regional basis there are significant radiogenic ^{4}He fluxes from the ocean sediment into the water column. Such features are not unexpected because at certain locations the seafloor is closer to the composition of continental crust than oceanic crust. However, averaged over the entire ocean basins, the flux of crustal ^{4}He is small compared to that from the continental crust.

Well et al. (2001) evaluated high-quality data from the Pacific Ocean that became available during the World Ocean Circulation Experiment (WOCE). Separating the crustal ^{4}He component from the mantle component, they revealed widespread occurrence of a crustal radiogenic ^{4}He flux out of deep-sea sediments and the oceanic crust into the water column (Fig. 9). Although the flux of ^{4}He is small in these regions, Well et al. (2001) were able to estimate a flux of roughly $1\pm0.4\times10^5$ atoms cm^{-2} s^{-1}. Further evaluation of the WOCE helium isotope and neon data will hopefully improve our knowledge on the distribution of helium sources and their relative flux values in the global ocean.

^{3}He

After the discovery of mantle-derived helium in the oceans (Clarke et al. 1969), the first estimate of the ^{3}He flux yielded a value of about 2 atoms cm^{-2} s^{-1} (Clarke et al. 1969). This estimate was based on simple advection/diffusion or straight advection models that utilize the mean concentration of excess ^{3}He in the deep waters of the ocean (Δ^3He) and mean residence time of the deep waters. The flux of this mantle-derived helium is concentrated in areas of active mid-ocean ridge spreading or ocean islands (e.g., Craig and Lupton 1981). Later estimates by Craig et al. (1975) were based on a larger, although still sparse, data set. In their new assessment of the ^{3}He flux from the ocean, these authors use two methods: one based on the average mean upwelling rate and the mean ^{3}He excess in the deep ocean, the other based on the ^{4}He flux and the ^{3}He/^{4}He ratio of the excess helium calculated from profiles located on the East Pacific Rise. They obtain values of 3.3 atoms cm^{-2} s^{-1} and 4.8 atoms cm^{-2} s^{-1}, respectively (average value given by Craig et al. 1975: 4 ± 1 atoms cm^{-2} s^{-1}.

Since these estimates of ^{3}He fluxes in the mid-1970s, little work has been done that would have resulted in significant refinements of these fluxes. Simulations of the mantle helium distribution using a global general ocean circulation model (Farley et al. 1995) used a simple parameterization of the ^{3}He flux from mid-ocean ridges and determined the

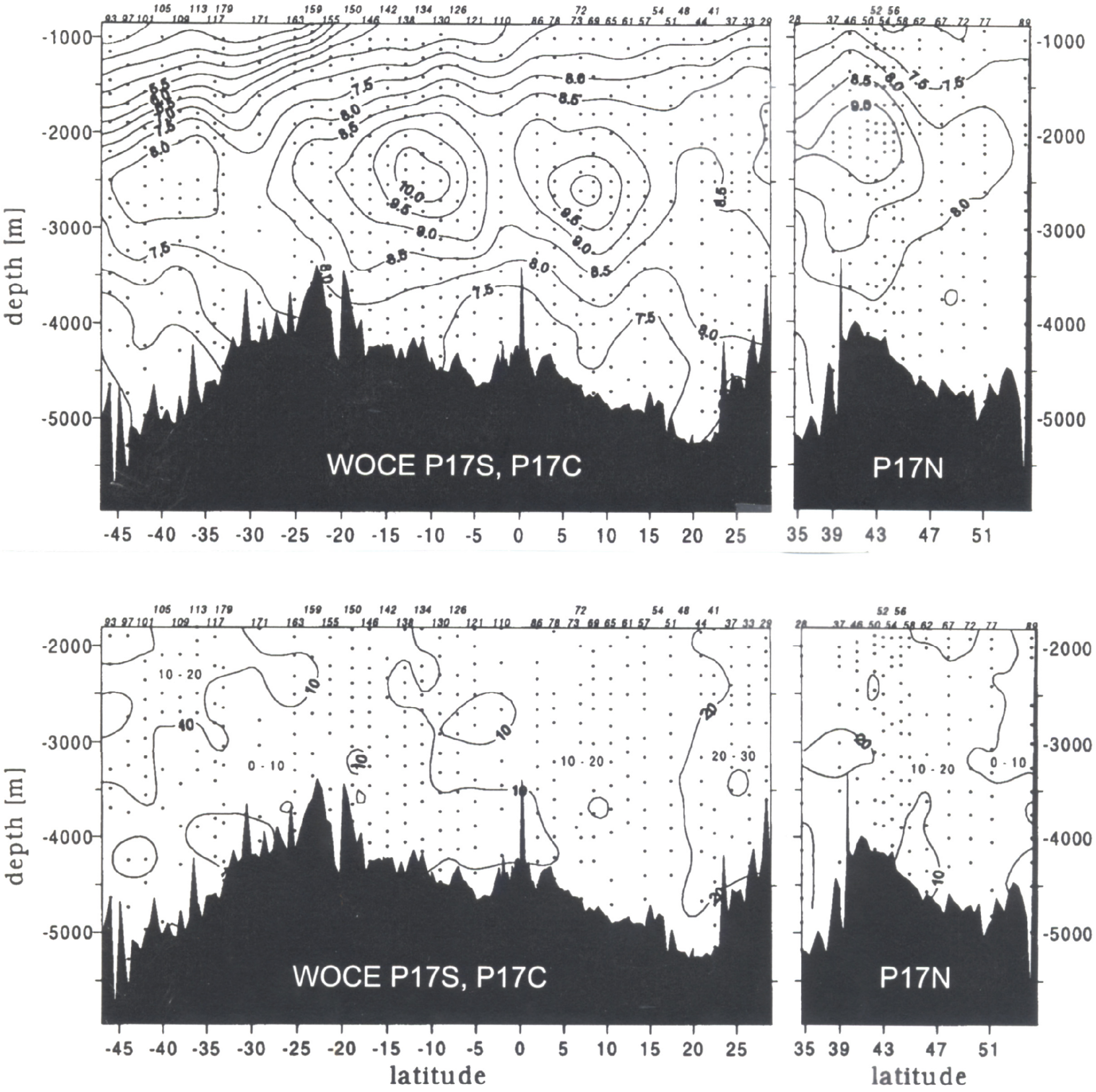

Figure 9. Distribution of the total ^{4}He excess (Δ^4He, in percent) along WOCE section P17 at 135°W in the Pacific Ocean (upper panels). The data can be used, together with measurements of neon and the ^{3}He/^{4}He ratio, to determine the fraction of radiogenic ^{4}He (in pmol kg^{-1}) contained in the deep waters below ~2000 m (lower panels). The data indicate the presence of a small radiogenic ^{4}He component in the deep and bottom waters of the Pacific Ocean. From Well et al. (2001).

distribution of the ^{3}He emanated from these sources throughout the world ocean. These simulations showed that with the specific source parameterization used in their study, Farley et al. (1995) could reproduce the global oceanic balance of ^{3}He reasonably well. However, at the same time the simulations clearly revealed that there is still much work to be done to understand the details of the simulated fields. Comparison with high-density surveys of ^{3}He in the ocean that are now becoming available (e.g., Lupton 1998, Rüth et al 2000) will enable us to reach a deeper level of understanding of the ^{3}He patterns observed in the ocean. Such progress should make new efforts to refine the estimate of the oceanic ^{3}He flux a worthwhile exercise.

EXTRATERRESTRIAL ^{3}HE IN DEEP-SEA SEDIMENTS

Delivery of extraterrestrial ^{3}He to the ocean sediments

Four decades ago, ^{3}He of apparent extraterrestrial origin was identified in ocean sediments. Merrihue (1964) observed ^{3}He/^{4}He ratios in marine sediments roughly 2 orders of magnitude higher than those observed in atmospheric helium and attributed it to the presence of cosmic material.

Systematic studies of noble gases in marine sediments were started in the early 1980s by Ozima et al. (1984). Shortly thereafter, Takayanagi and Ozima (1987) recognized the potential of ^{3}He as a proxy of sediment accumulation rates. Most studies of noble gases in marine sediments (including this chapter) focus on helium isotopes, however, neon (Nier and Schlutter 1990, 1993) and argon isotopes (Tilles 1966, 1967; Amari and Ozima 1988) have also been studied. In the early 1990s, extraterrestrial ^{3}He in ocean sediments received considerable attention when Anderson (1993) questioned the understanding of mantle geochemistry and proposed that the mantle ^{3}He might not represent volatiles trapped in the earth in early earth history but rather is derived from subducted interplanetary dust particles (IDPs). However, this hypothesis could be refuted based on mass flux considerations (Allègre et al. 1993) and experimental evidence showing that helium would not be retained during subduction due to sufficiently high diffusion coefficients (Hiyagon 1994).

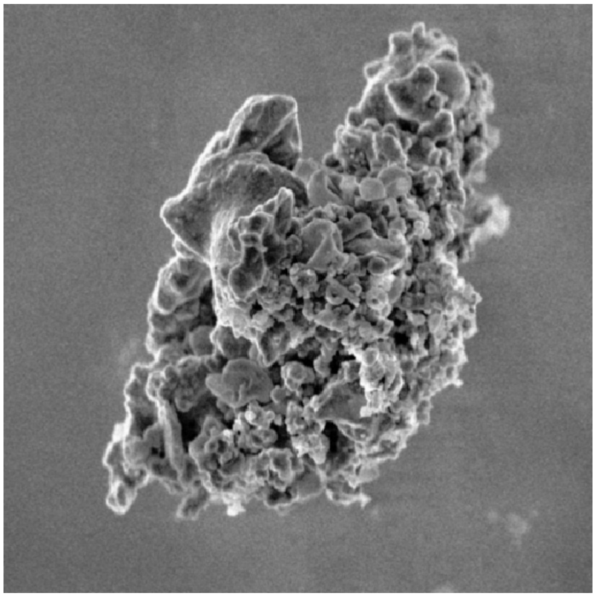

Figure 10. Electron microscope picture of an interplanetary dust particle. The size of the particles carrying the extraterrestrial ^{3}He that are accumulated in marine sediments typically is between 3 and 35 μm (e.g., Farley et al. 1997) [photograph courtesy of Scott Messenger, http://stardust.wustl.edu].

Extraterrestrial ^{3}He is delivered to the earth surface by interplanetary dust particles (IDP, Fig. 10). IDPs are derived from asteroid collisions as well as cometary debris (Dohnanyi 1976) and are thought to acquire their characteristic helium signature from implantation of solar wind and solar flare gases (e.g., Nier and Schlutter 1990). Approximately 40,000 tons of IDPs are deposited annually on the earth's surface (Love and Brownlee 1993). However, the major fraction of the IDPs is heated to temperatures >800°C during entry into the earth's atmosphere and looses its helium signal (Farley et al. 1997). Only IDPs with diameters ≤ 35 microns, corresponding to 0.5% of the total IDP mass flux, transit the atmosphere at temperatures of 500-800°C or below (Fraundorf et al. 1982) and retain their extraterrestrial helium signature. After being removed from the troposphere mainly by wet deposition and rapid settling through the oceanic water column, the IDPs continuously accumulate in marine sediments (e.g., Takayanagi and

Ozima 1987) or on ice shields (Brook et al. 2000).

The helium isotope characteristics of IDPs are well constrained from analysis of individual particles collected from the stratosphere. They have a $^3He/^4He$ ratio of 2.4×10^{-4}, as well as a fairly constant ^3He concentration of 1.9×10^{-5} cm^3 STP g^{-1} (Nier and Schlutter 1992). As the cosmic dust is enriched in ^3He by ~8 orders of magnitude compared to terrigenous matter it can be readily detected. However, in spite of various noble gas studies of single IDP grains, both from the stratosphere and ocean sediments (e.g., Fukumoto et al. 1986; Nier et al. 1990; Nier and Schlutter 1992) the carrier phase that actually hosts the extraterrestrial helium has not been unambiguously identified. Amari and Ozima (1985) found that the helium resides mainly in the magnetic fraction of sediments and therefore identified magnetite to be the main carrier of the extraterrestrial ^3He signal. The magnetite is thought to be produced by heating of the IDPs during atmospheric entry (Amari and Ozima 1985). In a subsequent study, Fukumoto et al. (1986) found significant helium contributions from a non-magnetic fraction and suggested extraterrestrial silicates to be another likely host mineral. The presence of a non-magnetic carrier phase was later confirmed by Patterson et al. (1998) and Farley (2001). Future work is needed to identify the relative importance of different carrier phases and whether they are associated to magnetic and/or non-magnetic sediment fractions.

The extraterrestrial helium signal is extremely well preserved in marine and terrestrial sedimentary archives over geological time scales. Various studies have shown that the extraterrestrial helium carried to the seafloor by IDPs can be retained for periods of at least 65 million years (Ma) against diffusive and/or diagenetic loss (Farley 1995; Farley et al. 1998). Recently, Patterson et al. (1998) identified extraterrestrial ^3He in 480-Ma old sedimentary rocks.

Helium contained in ocean sediments can be interpreted as a mixture of helium from two sources, extraterrestrial and terrigeneous helium (Takayanagi and Ozima 1987; Marcantonio et al. 1995). Contributions from an atmospheric helium component have been shown to be negligible (e.g., Farley and Patterson 1995). Assuming that the isotopic compositions of both mixing end-members are known, one can easily calculate the amount of extraterrestrial ^3He, using the following equation:

$$\frac{^3He_{ET}}{^3He_m} = \frac{1 - \dfrac{\left(\dfrac{^3He}{^4He}\right)_{ter}}{\left(\dfrac{^3He}{^4He}\right)_m}}{1 - \dfrac{\left(\dfrac{^3He}{^4He}\right)_{ter}}{\left(\dfrac{^3He}{^4He}\right)_{ET}}} \tag{6}$$

where *m* denotes the measured, *ET* the extraterrestrial, and *ter* the terrigeneous component. Whereas the extraterrestrial IDP component is well constrained ($^3He/^4He = 2.4\times10^{-4}$, $[^3He] = 1.9\times10^{-5}$ cm^3 STP g^{-1}, Nier and Schlutter 1992), the helium isotope composition of the terrigeneous end-member is less well constrained and may vary regionally depending on the age and composition of the source material (Marcantonio et al. 1998; Farley 2001). A series of mixing lines that have the extraterrestrial component as one end-member and fan out towards different terrigeneous end-members can be drawn (Fig. 11). In regions of low terrigeneous supply (i.e., far away from ocean-margin sites and volcanic input) such as the central and eastern equatorial Pacific where most of the work on extraterrestrial ^{3}He in deep-sea sediments has been conducted, ^{3}He/^{4}He ratios range from 10^{-5} to 10^{-4} (Marcantonio et al. 1995, 1996; Patterson and Farley 1998; Winckler et al. 2001b) and virtually all ^{3}He (>99.5%) is of extraterrestrial origin. Here, the choice of the ^{3}He/^{4}He ratio of the sedimentary end-member is not very critical and does not significantly change the mixing lines. Typical IDP concentrations in sediments that are not diluted by a terrigeneous component are of the order of 0.1 to 1 ppm; in sediments dominated by terrigeneous components they can be lower than 1 ppb.

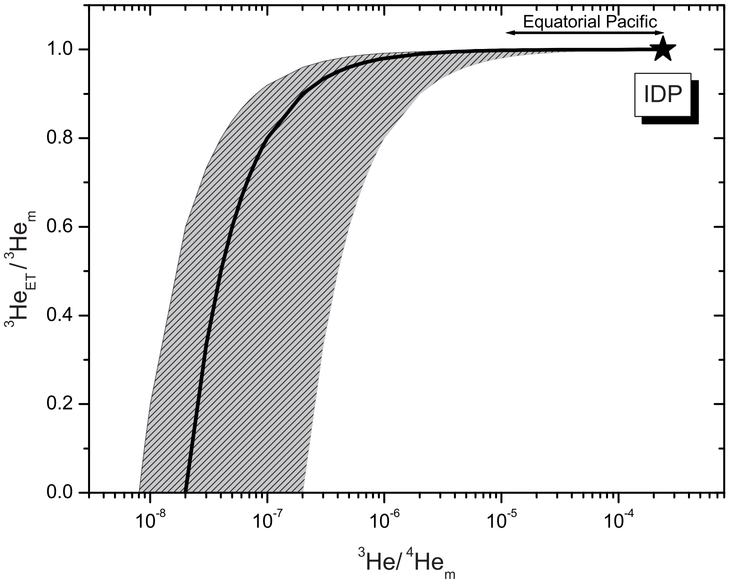

Figure 11. Relative fraction of extraterrestrial ^{3}He in the total observed ^{3}He concentration of a sediment sample plotted versus the ^{3}He /^{4}He ratio (modified from Farley 2001). The heavy black line represents mixing of an IDP component and an average terrigeneous component (^{3}He/^{4}He = 2×10^{-8}, e.g., Farley and Patterson 1995). The envelope represents mixing with the two extreme cases of terrigeneous helium signatures analyzed to date: sediments derived from old continental crust (e.g., North Atlantic ice-rafted debris with ^{3}He/ ^{4}He = 6×10^{-9}, Marcantonio et al. 1998) and sediments from the Amazon River fan (^{3}He/^{4}He = 2×10^{-7}, Marcantonio et al. 1998).

Applications of IDP-derived ^{3}He

Following the pioneering work by Takayanagi and Ozima (1987) several recent studies have investigated extraterrestrial ^{3}He in sediments over times scales of thousands to tens of millions of years, both to constrain sedimentation rates in paleoceanographic studies and variations of the IDP accretion to obtain astrogeophysical information.

The Cenozoic record. Farley and coworkers used the extraterrestrial ^{3}He signal in marine sediments to study astrogeophysical events (for a review, see Farley 2001). In a 70 Ma record from the central North Pacific, they identified ^{3}He flux variations and attributed them to asteroidal breakup events or the passage of comets through the inner solar system (Farley 1995). In a more detailed study focusing on the Late Eocene they found evidence for large comet shower impact events in the Late Eocene by tracing the IDP fluxes associated with them (Farley et al. 1998).

The Quaternary record. Studies of Pleistocene sediments from the North Atlantic and the equatorial Pacific revealed that the accumulation of extraterrestrial ^{3}He exhibits a strong cyclicity with a period of ~100 ka (Farley and Patterson 1995; Marcantonio et al.

1995, 1996, 2001; Patterson and Farley 1998; for an example see Fig 12). However, the interpretation of those sediment records is still controversial. Interestingly, both interpretations link the ^{3}He signal to climate change:

- Farley and Patterson (1995) and Patterson and Farley (1998) interpreted the variability of the ^{3}He accumulation in deep-sea sediments to directly reflect the cyclicity of the accretion rate of IDPs, i.e. changes in delivery of IDPs from space. This interpretation supports a recent hypothesis by Muller and MacDonald (1995, 1997a,b,c) that the accretion rate of cosmic dust to the earth varies with the 100 ka cycle of Earth's inclination and may be responsible—in contrast to the widely accepted Milankovitch theory—for forcing the 100 ka climate cycle.

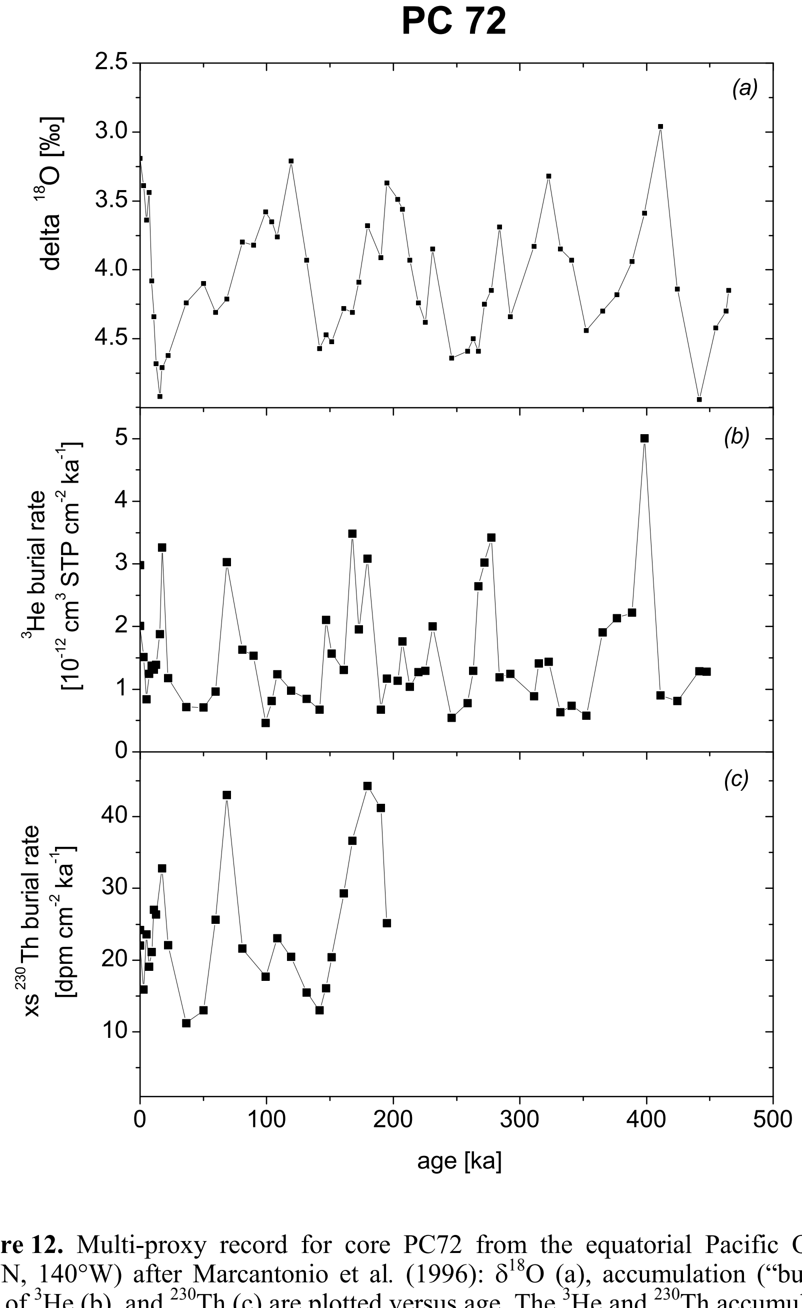

Figure 12. Multi-proxy record for core PC72 from the equatorial Pacific Ocean (0.1°N, 140°W) after Marcantonio et al. (1996): δ^{18}O (a), accumulation ("burial") rates of ^{3}He (b), and ^{230}Th (c) are plotted versus age. The ^{3}He and ^{230}Th accumulation rates are derived by multiplying the concentrations with the ^{18}O-derived bulk sedimentation rates and show synchronous 100 kyr variability.

- Marcantonio et al. (1995, 1996, 2001) reached a different conclusion. These authors compared the ^{3}He record to that of ^{230}Th$_{ex}$, which is well established as a constant flux tracer due to its homogeneous production in the water column and its high particle reactivity (e.g., François et al. 1990). Both records show a strong correlation for the last 210 ka. Given that both tracers are derived from a different and decoupled source, the small variability in the ^{3}He/^{230}Th$_{ex}$ ratio is a strong indication that the flux of IDPs and consequently extraterrestrial ^{3}He to the seafloor has been constant during that period. Marcantonio et al. (1995, 1996, 2001) postulate that the variability of the ^{3}He accumulation is caused by variable sediment redistribution by deep-sea currents, so-called sediment focusing. The focusing patterns are correlated with the global climate record such that periods of maximum focusing correspond to interglacials leading to the hypothesis that the temporal pattern of sediment accumulation reflects climate-related reorganization of deep-sea currents (Fig.12).

Potential of ^{3}He as a constant flux tracer. Marcantonio et al.'s (1995, 1996, 2001) findings and interpretation open up the potential of IDP-derived extraterrestrial ^{3}He as a constant flux proxy. In various recent studies, the ^{3}He flux has been determined independently. The estimate of Marcantonio et al. (1996, 2001) for the ^{3}He$_{ET}$ flux in the equatorial Pacific ($8.0 \pm 2.4\times10^{-13}$ cm^3 STP cm^{-2} ka^{-1}) is in agreement with the global average Holocene ^{3}He$_{ET}$ flux ($7.7 \pm 2\times10^{-13}$ cm^3 STP cm^{-2} ka^{-1}) reported by Higgins (2001) and the ^{3}He$_{ET}$ flux determined from ice core studies ($6.2\pm2.7\times10^{-13}$ cm^3 STP cm^{-2} ka^{-1} for Greenland/GISP2 and $7.7\pm2.5\times10^{-13}$ cm^3 STP cm^{-2} ka^{-1} for Vostok, Brook et al. 2000). Further support for this approach on even longer timescales is derived from comparative studies of ^{3}He and ^{10}Be in the Pacific Ocean confirming a constant ^{3}He delivery to the earth over 7 Ma (Higgins 2001). However, there is clearly a need for more calibration work to unambiguously confirm the constancy of the ^{3}He$_{ET}$ flux over these time scales and thus to finally establish the use of ^{3}He as constant flux tracer.

In the paleo-oceanographic context, constant flux tracers are valuable tools because they enable the reconstruction of particulate fluxes. One of the advantages of this approach is that it allows us to establish mass accumulation rates independently from single-point age models (e.g., ^{18}O). These models frequently are biased and sensitive to sediment redistribution effects. For example, this holds true for paleoceanographic studies in the Quaternary, where many interpretations of the sediment record rely on potentially erroneous sediment accumulation rates derived from δ^{18}O stratigraphy.

Under the assumption of a constant ^{3}He flux ($F_{^3He}$) the instantaneous mass sediment accumulation rate (MAR) is inversely proportional to the ^{3}He concentration

$$\mathrm{MAR} = \frac{F_{^3\mathrm{He}}}{^3\mathrm{He}} \tag{7}$$

Accordingly, the particle fluxes (AR) of other sedimentary components i are

$$\mathrm{AR}_{\,\mathrm{i}} = \mathrm{MAR}\cdot[\mathrm{i}] = \frac{F_{^3\mathrm{He}}}{^3\mathrm{He}}\cdot[\mathrm{i}] \tag{8}$$

Unlike the Thorium method, which is limited to the past 250 ka due to radioactive decay, ^{3}He, a stable isotope, should be useful as a constant flux proxy on longer time scales.

Whereas there is an ongoing controversy about application of the constant flux proxy approach for Pleistocene records (see above), there is agreement (Farley et al. 2001) about the recently developed application of the method to determine the duration of 'special' extreme events in the geological past. Mukhopadhyay et al. (2001) used the constant flux characteristics of ^{3}He to determine the time interval over which the deposition of the K/T boundary clay occurred to be 11±2 ka. Eltgroth and Farley (2001) used a similar approach to evaluate the duration of the Late Paleocene Thermal Maximum.

NOBLE GASES IN DEEP-SEA BRINES

Deep-sea brines are hypersaline water bodies that have been observed in various deep-sea environments, such as the Red Sea, the eastern Mediterranean and the Gulf of Mexico. Their high salt concentrations (up to 15 times the concentration of seawater) are attributed to leaching of underlying evaporites. Due to their high density, they are typically found in depressions on the seafloor, so-called brine basins. Noble gases have proven to be valuable tools to decode the complex geochemical processes underlying the origin and formation of these brines.

The Red Sea

In 1966, Miller et al. (1966) discovered the first deep-sea brine, the Atlantis II brine, in the central rift zone of the Red Sea, which contains more than 20 morphological depressions filled by highly saline brines (Hartmann et al. 1998). The brines are part of the geological setting of the Red Sea: whereas the southern part is a young spreading center, the northern part is tectonically inactive. Noble gas studies have significantly contributed to understanding the origin and evolution of these deep-sea brine systems. Lupton et al. (1977) detected MORB-derived helium ($^3He/^4He = 1.2\times10^{-5}$) and demonstrated that the Atlantis II brine is part of an active hydrothermal system below the Red Sea. In a more detailed study in the late 90s, elevated $^{40}Ar/^{36}Ar$ ratios up to 305 (compared to 295.5 for atmospheric $^{40}Ar/^{36}Ar$ ratios) were identified in the Atlantis II brine confirming the transport of mantle-derived argon in hydrothermal fluids along with mantle-derived helium at active seafloor hydrothermal systems (Winckler et al. 2001a). The hydrothermal activity is thought to accompany the recent start of seafloor spreading in the transition zone between the Southern and Northern Red Sea (Bonatti 1985).

Systematic studies of atmospheric noble gases were used to reconstruct the dynamic processes underlying the formation of the Atlantis II brine. The atmospheric noble gases (Ne, Ar_{atm}, Kr, Xe) in the deepest brine layer of the Atlantis II brine were found to be depleted by 20-30% compared to the initial concentrations in ambient Red Sea Deep Water. No systematic fractionation between the different noble gases was observed, which suggests sub sea floor boiling and subsequent phase separation to be responsible for the observed depletion pattern (Winckler et al. 2000). Together with the MORB characteristics of the helium and argon isotopes, the geochemical evolution of the brine before injection into the deep water could be reconstructed. After having circulated through evaporites, where it became enriched in salt, and through young oceanic crust, where it became enriched in MORB derived helium and argon, the ascending fluid boils, and consequently the residual liquid is depleted in atmospheric noble gases. The depleted fluid rises to the sediment surface and feeds the Atlantis II brine system. The noble gas study of Winckler et al. (2000) provides evidence that the Red Sea brines are oceanic hydrothermal systems, similar to vent systems at sediment-free ridges (e.g., the Juan de Fuca Ridge), where boiling and phase separation control the hydrothermal chemistry.

Extending the study of the Red Sea brines to the inactive northern part, Winckler et al. (2001a) observed significant differences of the helium and argon isotope characteristics along the Red Sea rift system. The Kebrit brine, located in the northern Red Sea, has a low helium isotope signature ($^3He/^4He = 1\times10^{-6}$) indicating a predominantly crustal origin and no signs of active hydrothermal input. The "radiogenic" signature is interpreted as the result of a helium flux from the continental crust that accumulates in the brine. Again, this is consistent with the geological setting of the northern part of the Red Sea where the continental crust is stretched and thinned representing pre-seafloor spreading conditions. The striking agreement of the geochemical fingerprints and the tectonic situation of the Red Sea, i.e. the northward progression of the seafloor spreading, confirms the unique potential of noble gases to contribute to the study of complex geochemical processes (Fig 13).

The Eastern Mediterranean

The Eastern Mediterranean is the site of 5 deep-sea basins that were discovered in the 1980s (e.g., Jongsma et al. 1983) and 1990s (MEDRIFF-Consortium 1996). Detailed noble gas studies were completed in three of them, the Urania, Atalante and Discovery brines, in order to investigate their origin and fluid kinematics.

In the Urania Basin, extraordinary helium and argon signatures were observed. The ^{4}He concentration of this brine is enriched by 4 to 5 orders of magnitude compared to ambient seawater. Low ^{3}He/^{4}He ratios of 1×10^{-7} and high ^{40}Ar/^{36}Ar ratios of up to 470 indicate a radiogenic source. On the basis of these data, Winckler et al. (1997) concluded that the Urania Basin is fed by advective transport from a deep fluid reservoir below the evaporite sequence that efficiently seals the crustal flux from lower sedimentary strata. The unique enrichment in ^{4}He is explained by a helium accumulation process over several million years, likely since the formation of the evaporites during the Messinian salinity crisis 6 Ma ago. Due to its extremely high ^{4}He concentration, injection of radiogenic helium from local features like the Urania brine may contribute significantly to the helium inventory and may be responsible for the high radiogenic helium excess (~6% compared to ambient sea water) in the deep (>1200 m) eastern Mediterranean (Roether et al. 1992, 1994, 1996). The case of the Urania Brine emphasizes the potential importance of brines as interface between local geochemical and oceanographic features on a regional scale.

AIR/SEA GAS EXCHANGE STUDIED BY DUAL TRACER RELEASE EXPERIMENTS

Background

Knowledge of air/sea gas exchange rates is central to understanding the balances and fluxes of a significant number of gases with impact on climate or biogeochemical cycles. They include dissolved O_2, CO_2, dimethyl sulphide (DMS), nitrous oxide, halocarbons, or methane (Bange et al. 1996; Bates et al. 1996; Blake et al. 1997; Liss 1999). These compounds may influence atmospheric chemistry and/or affect atmospheric ozone levels. They also might contribute to climate change (Hahn and Crutzen 1982; Charlson and Rodhe 1982; Charlson et al. 1987; Solomon et al. 1994). Due to the great difficulty in direct measurement of the gas transfer rate between the ocean and the atmosphere, considerable uncertainty still exists in the balances and air/sea fluxes for these gases. Early measurements of the air/sea gas exchange rates were focused on the ^{14}C and ^{222}Rn methods (Roether and Kromer 1978; Broecker and Peng 1982; Smethie et al. 1985). Fundamental methodological problems with these methods led to the development and application of dual gas tracer experiments. In these experiments, two inert gases with similar solubility and different diffusion coefficients are injected into a near-surface water body and the change in the ratio of the gases due to gas exchange across the molecular boundary layer is converted into gas transfer coefficients. Measurement of the ratio of two gases avoids some of the difficulties with inhomogeneities in the tracer distributions in the water that affected the ^{222}Rn method and the large scale averaging that was used for the ^{14}C method. The most widely used tracers are ^{3}He in combination with SF_6.

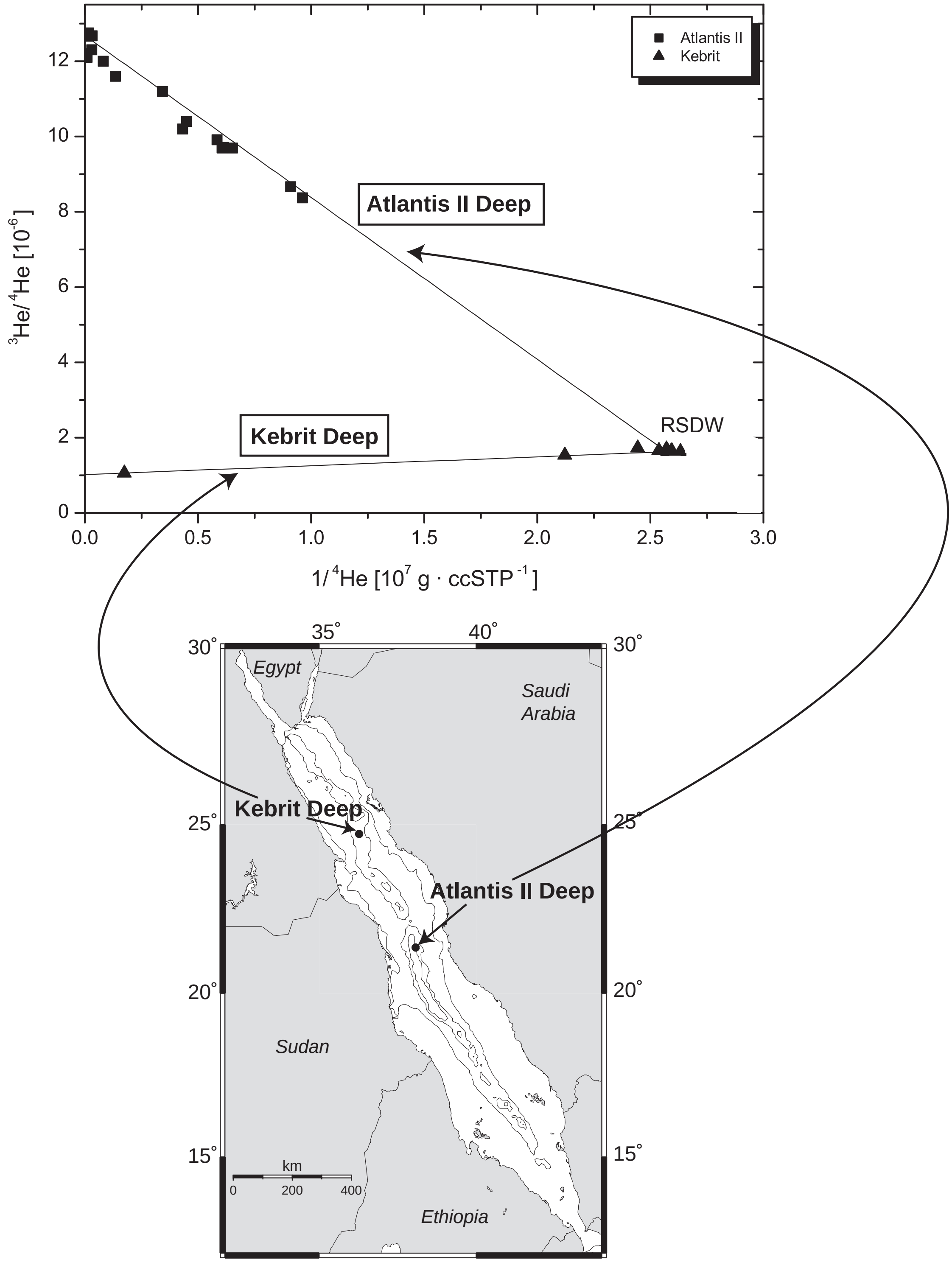

Figure 13. Correlation of ^{3}He/^{4}He with reciprocal of ^{4}He concentration (1/^{4}He) from two brine basins in the Red Sea after Winckler et al. (2001a). Samples from the Atlantis brine define a mixing between RSDW (Red Sea Deep Water) and a MORB-derived component (^{3}He/^{4}He = 1.27×10^{-5} = 9.2 R_a), samples from Kebrit brine lie on a mixing line between RSDW and a ^{4}He-enriched 'crustal' end-member (^{3}He/^{4}He = 1×10^{-6}). The different helium isotopic fingerprints of the two brines reflect the geological setting, i.e., the northward progression of seafloor spreading in the Red Sea.

$SF_6/^3He$ Method

Dispersion and gas exchange rates in unconfined natural water systems can be determined using two volatile gaseous tracers with different gas exchange rates if the ratio of the gas exchange rates is known. The gas exchange rate of a gas is proportional to the Schmidt number (defined as the kinematic viscosity of water divided by the molecular diffusivity of the gas in water) of the gas raised to an exponent *n* (Jähne et al. 1987). For wavy, unbroken water surfaces without bubble entrainment, *n* has been shown to be -0.5 in both laboratory experiments (Jähne et al. 1984; Ledwell 1984; Asher et al. 1992) and field measurements (Watson et al. 1991). Under these conditions, the ratio of *k* for SF_6 and ^3He can be expressed as:

$$\frac{k_{SF_6}}{k_{^3He}} = \left(\frac{Sc_{SF_6}}{Sc_{He}}\right)^{-0.5} \tag{9}$$

where k_{SF6} and k_{3He} are the gas exchange rates of SF_6 and ^3He, Sc_{SF6} and Sc_{3He} are the Schmidt numbers for SF_6 and ^3He, respectively. The gas exchange rate of ^3He can be determined by combining the advection-diffusion equation for ^3He and SF_6 in water and incorporating Equation (9):

$$k_{^3He} = h\frac{d}{dt}\left(\frac{\ln\left(^3He/SF_6\right)}{1-\left(Sc_{SF_6}/Sc_{^3He}\right)^{-0.5}}\right) \tag{10}$$

where *h is* the average water depth, -0.5 is the Schmidt number exponent, and ^3He and SF_6 are the excess of ^3He and SF_6 in the mixed layer. Conversely, k_{SF6} can be determined by substituting SF_6 for ^3He and vice versa in Equation (10). After separating the gas exchange component, the dispersion can be accounted for with a method described by Clark et al. (1996).

Results from oceanic dual gas tracer releases

The dual gas tracer method (typically ^3He and SF_6) has been used to study gas exchange in rivers/estuaries (e.g., Clark et al. 1994), the coastal ocean (e.g., Watson et al. 1991; Wanninkhof et al. 1993; Wanninkhof et al. 1997; Nightingale et al. 2000a), and the open ocean (Nightingale et al. 2000b). For such experiments, mixtures of ^3He and SF_6 are injected into the surface waters and the decrease of the $^3He/SF_6$ ratio is monitored as a function of time and wind speed. Results from an experiment on Georges Bank indicate that the method can provide valuable data that yield gas exchange rates averaged over periods of several days. During the course of the experiment the $^3He/SF_6$ ratio decreased by a factor of about 3 over a period of 8 days due to gas loss to the atmosphere (Fig. 14); ^3He escapes much faster than SF_6 due to its higher diffusion coefficient in the molecular boundary layer. The measured $^3He/SF_6$ ratios were translated into gas transfer coefficients using Equation (10). The resulting gas transfer coefficients provided valuable information on the relationship between gas transfer velocities and wind speed (Fig. 15). For a long time, this relationship was very poorly defined and even today there are still large gaps in our understanding of air/sea gas exchange, as well as in our capability to measure the variables that would define it better.

PERSPECTIVES

Noble gases have been firmly established as routine tools in studies of a variety of oceanographic fields. Since the first pioneering measurements of noble gases in the ocean and its sedimentary environment, rich data sets, some of them with global coverage at high spatial resolution, were collected and evaluated. In many cases such as the application of tritium/^3He and mantle ^3He to ocean circulation, detailed descriptions of

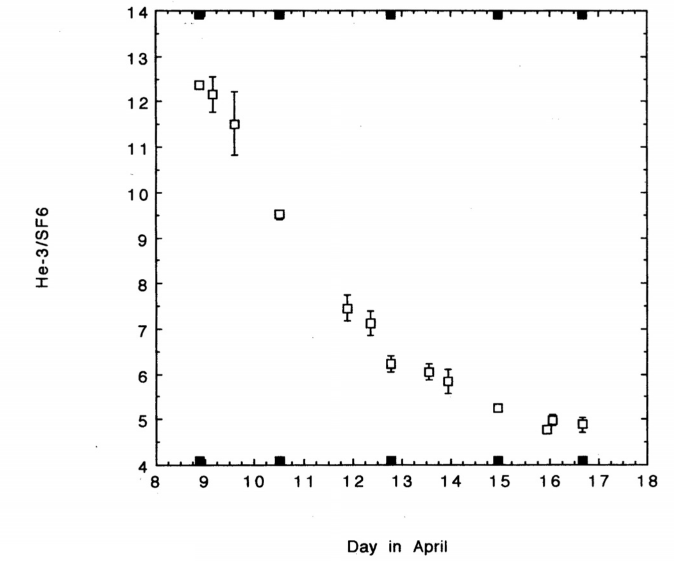

Figure 14. Change in $SF_6/^3He$ ratio over time during the gas transfer experiment on Georges Bank. From Wanninkhof et al. (1993).

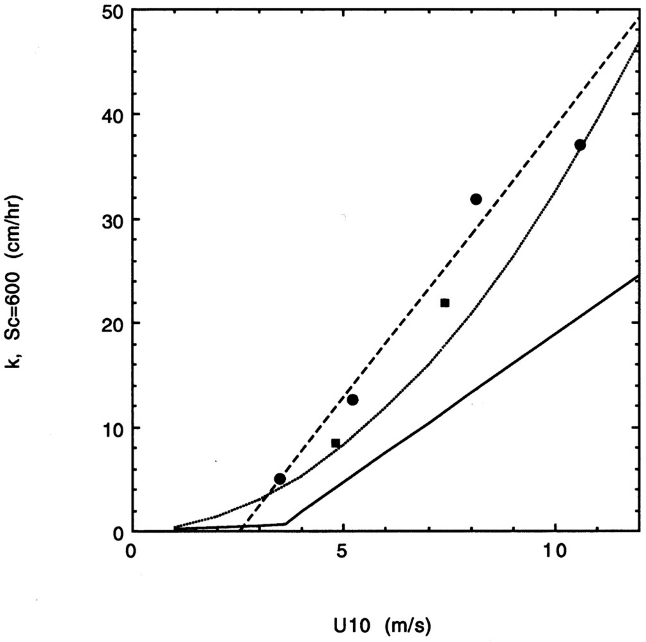

Figure 15. Relationship between gas transfer velocity k (normalized to a Schmidt number of 600) and wind speed u (normalized to 10-m height). Data from $SF_6/^3He$ experiment (circles) are shown in comparison to the relationships proposed by Liss and Merlivat (1986, solid line), Wanninkhof (1992, dotted) and Smethie et al. (1985, dashed). From Wanninkhof et al. (1993).

the tracer fields consisting of several tens of thousands of measurements were obtained mainly during the 1990s in the framework of the WOCE. Synthesis and analysis of these data is underway and will contribute to our understanding of the formation, circulation and variability of oceanic water masses. They are increasingly used in model calibration efforts and they guide future sampling campaigns. Although the tritium signal is decreasing in the oceans due to the spike-type delivery of tritium with the main peak having occurred in the early 1960s, as well as the radioactive decay of tritium, there is still a sufficiently large signal left to obtain a signal to noise ratio of ~100 in the northern hemisphere. It is anticipated that tritium/^3He will yield valuable information on ocean circulation that is complementary to that obtained from other methods, including transient tracers such as the CFCs (chlorofluorocarbons) CFC 11, CFC 12, and CFC 113. Other applications of noble gases to oceanographic studies are still in the stage of establishing and firming up the methodology. For example, extraterrestrial ^3He in deep-sea sediments has shown potential as tracer for estimating sediment accumulation rates and first results have been obtained that show its value for paleoceanographic studies. The next steps in the development of this tracer have to be systematic surveys of deep-sea sediment cores and careful examination of the constancy of the ^{3}He flux to the sediment over long time scales. Similarly, the studies of deep-sea brines have shown the value of noble gases for such studies. Further results will reveal the full strength of these tracers in investigations of the origin and dynamics of such brines. The few coastal and open ocean ^{3}He/SF$_6$ release experiments showed that this method yields valuable results. Future applications should be integrated with direct flux measurements of the air/sea exchange that allow us to resolve short time scales (the ^{3}He/SF$_6$ experiments provide gas exchange rates averaged over longer time scales and larger space scales).

Future developments in Accelerator Mass Spectrometry might enable development of ^{39}Ar to a routine tool in oceanography. If the technical difficulties in measuring this noble gas isotope on small water samples can be mastered, it would offer a unique tool for studies of ocean circulation on time scales ranging from decades to the order of one thousand years, a good match for mean residence times of intermediate and deep waters (e.g., Loosli 1989).

Overall, during the past roughly four decades noble gases have significantly contributed to the field of oceanography. We anticipate that future studies will provide further extensive data sets that will form the foundation for improvement in our knowledge of a wide variety of topics. These topics reach from modern circulation of the ocean to understanding processes that shaped the oceanic environment over many millions of years.

ACKNOWLEDGMENTS

This chapter was written with support from the U.S. National Science Foundation (Grant # OCE 9820130) and the Deutsche Akademie der Naturforscher Leopoldina (Leopoldina Fellowship to G. Winckler). Comments by W. Aeschbach-Hertig and an anonymous reviewer considerably improved the manuscript. This is L-DEO contribution #6353.

REFERENCES

Allègre CJ, Sarda P, Staudacher T (1993) Speculations about the cosmic origin of He and Ne in the interior of the Earth. Earth Planet Sci Lett 117:229-233

Amari S, Ozima M (1985) Search for the origin of exotic helium in deep-sea sediments. Nature 317: 520-522

Amari S, Ozima M (1988) Extraterrestrial noble gases in deep-sea sediments. Geochim Cosmochim Acta 52:1087-1095

Anderson DL (1993) Helium-3 from the mantle: primordial signal or cosmic dust? Science 261:170-176

Asher WE, Farley PJ, Wanninkhof R, Monahan EC, Bates TS (1992) Laboratory and field measurements concerning the correlation of fractional area foam coverage with air/sea gas transport. *In* Precipitation Scavenging and Atmosphere-Surface Exchange, Vol. 2. SE Schwartz, WGN Slinn (eds) Hemisphere, p 815-828

Atakan Y, Roether W, Münnich KO, Matthess G (1974) The Sandhausen shallow-groundwater tritium experiment. *In* Isotope Techniques in Groundwater Hydrology (Proc Symp Vienna), Intl Atom Energy Agency, Vienna, p 21-43

Bange HW, Rapsomanikis S, Andreae MO (1996) Nitrous oxide emissions from the Arabian Sea. Geophys Res Lett 23:3175-3178

Bates TS, Kelly KC, Johnson JE, Gammon RH (1996) A re-evaluation of the open ocean source of methane to the atmosphere. J Geophys Res 101(D3):6953-6961

Begemann F, Libby WF (1957) Continental water balance, ground water inventory and storage times, surface ocean mixing rates and worldwide water circulation patterns from cosmic-ray and bomb tritium. Geochim Cosmochim Acta 12:277-296

Benson BB, Krause D (1980) Isotopic fractionation of helium during solution: A probe for the liquid state. J Solution Chem 9:895-909

Bieri RH, Koide M, Goldberg ED (1966) Noble gas contents of Pacific seawaters. J Geophys Res 71: 5243-5246

Blake NJ, Blake DR, Chen TY, Collins JE, Sachse GW, Anderson BE, Rowland FS (1997) Distribution and seasonality of selected hydrocarbons and halocarbons over the western Pacific basin during PEM-West A and PEM-West B. J Geophys Res 102(D23):28315-28331

Bönisch G, Schlosser P (1995) Deep water formation and exchange rates in the Greenland/Norwegian seas and the Eurasian Basin of the Arctic Ocean derived from tracer balances. Prog Oceanogr 35:29-52

Bönisch G, Blindheim J, Bullister JL, Schlosser P, Wallace DWR (1997) Long-term trends of temperature, and transient tracers in the central Greenland Sea. J Geophys Res 102:18553-18571

Bonatti E (1985) Punctiform initiation of seafloor spreading in the Red Sea during transition from a continental to an oceanic rift. Nature 316: 33-37

Broecker WS, Peng T-H (1982) Tracers in the Sea. Eldigio Press, Palisades, NY

Broecker WS, Peng T-H, Östlund HG (1986) The distribution of bomb tritium in the ocean. J Geophys Res 91:14331-14344

Brook EJ, Kurz MD, Curtice J, Cowburn S (2000) Accretion of interplanetary dust in polar ice. Geophys Res Lett 27:3145-3148

Butterfield DA, Massoth GJ, McDuff RE, Lupton JE, Lilley MD (1990) Geochemistry of hydrothermal fluids from Ashes Vent Field, Axial Seamount, Juan de Fuca Ridge: Sub-seafloor boiling and subsequent fluid-rock interaction. J Geophys Res 95(B8):12895-12921

Charlson RJ, Rodhe H (1982) Factors controlling the acidity of natural rainwater. Nature 295:683-685

Charlson RJ, Lovelock JE, Andreae MO, Warren SG (1987) Oceanic phytoplankton, atmospheric sulfur, cloud albedo and climate. Nature 326:655-661

Clark JF, Wannikhof R, Schlosser P, Simpson HJ (1994) Gas-exchange rates in the tidal Hudson River using a dual tracer technique. Tellus B 46:274-285

Clark JF, Schlosser P, Stute M, Simpson HJ (1996) SF_6-^{3}He tracer release experiment: a new method of determining longitudinal dispersion coefficients in large rivers. Environ Sci Techn 30:1527-1532

Clarke WB, Beg MA, Craig H (1969) Excess ^{3}He in the sea: Evidence for terrestrial primordial helium. Earth Planet Sci Lett 6:213-220

Clarke WB, Beg MA, Craig H (1970) Excess He-3 in East Pacific. EOS Trans Am Geophys Union 51: 325-326

Clarke WB, Jenkins WJ, Top Z (1976) Determination of tritium by mass spectrometric measurement of ^{3}He. Intl J Appl Rad Isotopes 27:515-522

Craig H, Lal D (1961) The production rate of natural tritium. Tellus 13:85-105

Craig H, Lupton JE (1981) Helium-3 and mantle volatiles in the ocean and the oceanic crust. *In* The Sea, Vol. 7. C Emiliani (ed) John Wiley & Sons, New York, p 391-428

Craig H, Weiss RF (1971) Dissolved gas saturation anomalies and excess helium in the ocean. Earth Planet Sci Lett 10:289-296

Craig H, Clarke WB, Beg MA (1975) Excess ^{3}He in deep water on the East Pacific Rise. Earth Planet Sci Lett 26:125-132

Dohnanyi JS (1976) Sources of interplanetary dust: Asteroids. *In* Interplanetary dust and zodiacal light 48:187-206. H Elsasser, H Fechtig (eds) Springer-Verlag, Berlin

Doney SC, Jenkins JW (1994) Ventilation of the deep western boundary current and abyssal western North Atlantic - Estimates from tritium and He-3 distributions. J Phys Oceanogr 24:638-659

Dreisigacker E, Roether W (1978) Tritium and ^{90}Sr in north Atlantic surface water. Earth Planet Sci Lett 38:301-312

Eltgroth SF, Farley KA (2001) High resolution timing of the Late Paleocene Thermal Maximum by extraterrestrial ^{3}He implied sedimentation rates at ODP site 690B. EOS Trans Am Geophys Union, Fall Mtg Suppl 82(:F1140

Farley KA (1995) Cenozoic variations in the flux of interplanetary dust recorded by ^{3}He in a deep-sea sediment. Nature 376:153-156

Farley KA (2001) Extraterrestrial helium in seafloor sediments: Identification, characteristics, and accretion rate over geological time. *In* Accretion of extraterrestrial matter throughout Earth's history. B Peucker-Ehrenbrink, B Schmitz (eds) Kluwer Academic/Plenum Publishers, p 179-204

Farley KA, Patterson DB (1995) A 100-kyr periodicity in the flux of extraterrestrial ^{3}He to the sea floor. Nature 378:600-603

Farley KA, Maier-Reimer E, Schlosser P, Broecker WS (1995) Constraints on mantle ^{3}He fluxes and deep-sea circulation from an oceanic general circulation model. J Geophys Res 100(B3):3829-3839

Farley KA, Love SG, Patterson DB (1997) Atmospheric entry heating and helium retentivity of interplanetary dust particles. Geochim Cosmochim Acta 61:2309-2316

Farley KA, Montanari A, Shoemaker EM, Shoemaker CS (1998) Geochemical evidence for a comet shower in the Late Eocene. Science 280:1250-1253

Farley KA, Mukhopadhyay S, Eltgroth S (2001) Assessment of the distribution of time in seafloor sediments using extraterrestrial ^{3}He. EOS Trans Am Geophys Union Fall Mtg Suppl 82:F1140

François R, Bacon MP, Suman DO (1990) ^{230}Th profiling in deep-sea sediments: high-resolution records of flux and dissolution of carbonate in the equatorial Atlantic during the last 24,000 y. Palaeoceanography 5:761-787

Fraundorf P, Lyons T, Schubert P (1982) The survival of solar flare tracks in interplanetary dust silicates on deceleration in the Earth's atmosphere. J Geophys Res 87:409-412

Fukumoto H, Nagao K, Matsuda J (1986) Noble gas studies on the host phase of high ^{3}He/^{4}He ratios in deep-sea sediments. Geochim Cosmochim Acta 50:2245-2253

Giletti BJ, Bazan F, Kulp JL (1958) The geochemistry of tritium. Trans Am. Geophys. Union 39:807-818

Grosse AV, Johnston WM, Wolfgang RL, Libby WF (1951) Tritium in nature. Science 113:1-2

Hahn J, Crutzen PJ (1982) The role of fixed nitrogen in atmospheric photochemistry. Phil Trans R Soc London, Ser B 296:521-541

Hartmann M, Scholten JC, Stoffers P, Wehner F (1998) Hydrographic structure of brine-filled deeps in the Red Sea: new results from the Shaban, Kebrit, Atlantis II and Discovery Deep. Mar Geol 144:311-330

Higgins S. (2001) Extraterrestrial tracer in the sea: evaluation and application of ^{3}He in interplanetary dust particles as a 'constant flux' tracer in marine sediments. PhD dissertation, Columbia University, New York, New York

Hiyagon H (1994) Retention of solar helium and neon in IDPs in deep sea sediments. Science 263: 1257-1259

Hohmann R, Schlosser P, Ludin A, Weppernig R (2002) Excess helium and neon in the Southeast Pacific: tracers for glacial meltwater. J Geophys Res (in press)

Jähne B, Huber W, Dutzi A, Wais T, Ilmberger J (1984) Wind/Wave-tunnel experiment on the Schmidt number and wave field dependence of air/water gas exchange. *In* Gas Transfer at Water Surfaces W Brutsaert, GH Jirka (eds) Reidel, Norwell, Massachusetts, p 303-309

Jähne B, Münnich KO, Bösinger R, Dutzi A, Huber W, Libner P (1987) On parameters influencing air-water gas exchange. J Geophys Res 92:1937-1949

Jenkins WJ (1974) Helium Isotope and Rare Gas Oceanology. PhD dissertation, McMaster University, Toronto, 170 p

Jenkins WJ (1982) Oxygen utilization rates in North-Atlantic sub-tropical gyre and primary production in oligotrophic systems. Nature 300:246-248

Jenkins WJ (1987) H-3 and He-3 in the Beta-Triangle: Observations of gyre ventilation and oxygen utilization rates. J Phys Oceanogr 17:763-783

Jenkins WJ (1996) Tritium and ^{3}He in the WOCE Pacific Programme. Intl WOCE Newslett 23:6-8.

Jenkins WJ (1998) Studying subtropical thermocline ventilation and circulation using tritium and He-3. J Geophys Res 103(C8):15817-15831

Jenkins WJ, Clarke WB (1976) The distribution of ^{3}He in the Western Atlantic Ocean. Deep-Sea Res. 23:481-494

Jongsma D, Fortuin AR, Huson W, Troelstra SR, Klaver GT, Peters JM, Van Harten D, De Lange GJ, Ten Haven L (1983) Discovery of an anoxic basin within the Strabo Trench, eastern Mediterranean. Nature 305:795-797

Kaufman S, Libby WF (1954) The natural distribution of tritium. Phys Rev 93:1337-1344

Kipfer R, Aeschbach-Hertig W, Peeters F, Stute M (2002) Noble gases in lakes and groundwaters. Rev Mineral Geochem 47:615-700

König H, Wänke H, Bien GS, Rakestraw NW, Suess HE (1964) Helium, neon and argon in the oceans. Deep-Sea Res. 11:243-247

Krylov AY, Mamyrin BA, Khabarin LA, Mazina TI, Silin YI (1974) Helium isotopes in ocean-floor bedrock, Geochem Int 11:839-844

Ledwell JR (1984) The variation of the gas transfer coefficient with molecular diffusivity. *In* Gas Transfer at Water Surfaces. W Brutsaert, GH Jirka (eds) Reidel, Norwell, Massachusetts, p 299-302

Liss PS (1999) Biogeochemistry - Take the shuttle-from marine algae to atmospheric chemistry. Science 285:1217-1218

Liss PS, Merlivat L (1986) Air-sea gas exchange rates: Introduction and synthesis. *In* The Role of Air-Sea Exchange in Geochemical Cycling. P Buat-Menard (ed) Reidel, Norwell, Massachusetts, p 113-129

Loosli HH (1989) Argon-39: A tool to investigate ocean water circulation and mixing. *In* Handbook of Environmental Isotope Geochemistry. P Fritz, J Ch Fontes (eds) Elsevier, Amsterdam, p 385-392.

Love SG, Brownlee DE (1993) A direct measurement of the terrestrial mass accretion rate of cosmic dust. Science 262:250-253

Lupton JE (1996) A far-field hydrothemal plume from Loihi Seamount. Science 272:976-979

Lupton JE (1998) Hydrothermal helium plumes in the Pacific Ocean. J Geophys Res 103:15853-15868

Lupton JE, Craig H (1975) Excess ^{3}He in oceanic basalts: evidence for terrestrial primordial helium. Earth Planet Sci Lett 26:133-139

Lupton JE, Craig H (1981) A major ^{3}He source at 15°S on the East Pacific Rise. Science 214:13-18

Lupton JE, Weiss RF, Craig H (1977) Mantle helium in the Red Sea brines. Nature 266:244-246

Lupton JE, Klinkhammer GP, Normark WR, Haymon R, Macdonald KC, Weiss RF, Craig H (1980) Helium-3 and manganese at the 21°N East Pacific Rise hydrothermal site. Earth Planet Sci Lett 50:115-127

Mamyrin BA, Tolstikhin IN (1984) Helium isotopes in nature. Elsevier, Amsterdam

Mamyrin BA, Tolstikhin IN, Anufriyev GS, Kamenskii IL (1969) Isotopic analysis of terrestrial helium on a magnetic resonance mass spectrometer. Geochem Intl 6:517-524

Marcantonio F, Kumar N, Stute M, Anderson RF, Seidl MA, Schlosser P, Mix A (1995) A comparative study of accumulation rates derived by He and Th isotope analysis of marine sediments. Earth Planet Sci Lett 133:549-555

Marcantonio F, Anderson RF, Stute M, Kumar N, Schlosser P, Mix A (1996) Extraterrestrial ^{3}He as a tracer of marine sediment transport and accumulation. Nature 383:705-707

Marcantonio F, Higgins S, Anderson RF, Stute M, Schlosser P, Rasbury ET (1998) Terrigeneous helium in deep-sea sediments. Geochim Cosmochim Acta 62:1535-1543

Marcantonio F, Anderson RF, Higgins S, Stute M, Schlosser P, Kubik P (2001) Sediment focusing in the central equatorial Pazific Ocean. Paleoceanography 16:260-267

MEDRIFF-Consortium (1996) Three brine lakes discovered in the seafloor of the eastern Mediterranean. EOS Trans Am Geophys Union 76:313

Merrihue C (1964) Rare gas evidence for cosmic dust in modern Pacific red clay. Ann. NY Acad. Sci. 119:351-367

Miller AR, Densmore CD, Degens ET, Hathaway JC, Manheim FT, McFarlin PF, Pocklington R, Jokela A (1966) Hot brines and recent iron deposits in deeps of the Red Sea. Geochim Cosmochim Acta 30: 341-359

Morison J, Steele M, Andersen R (1998) Hydrography of the upper Arctic Ocean measured from the nuclear submarine USS Pargo. Deep-Sea Res Part I 45:15-38

Morison J, Aagaard K, Steele M (2000) Recent environmental changes in the Arctic: A review. Arctic 53:359-371

Mukhopadhyay S, Farley KA, Montanari A (2001) A short duration of the Cretaceous-Tertiary boundary event: Evidence from extraterrestrial helium-3. Science 291:1952-1955

Muller RA, MacDonald GJ (1995) Glacial cycles and orbital inclination. Nature 377:107-108

Muller RA, MacDonald GJ (1997a) Glacial cycling and astronomical forcing. Science 277:215-218

Muller RA, MacDonald GJ (1997b) Spectrum of 100kyr glacial cycle: Orbital inclination, not eccentricity. Proc Nat Acad Sci USA 94:8329-8334

Muller RA, MacDonald GJ (1997c) Simultaneous presence of orbital inclination and eccentricity in proxy climate records from Ocean Drilling Program Site 806. Geology 25:3-6

Münnich KO, Roether W (1967) Transfer of bomb ^{14}C and tritium from the atmosphere to the ocean: Internal mixing of the ocean on the basis of tritium and ^{14}C profiles. *In* Radioactive dating and methods of Low Level Counting (Proc Symp Monaco), Intl Atom Energy Agency, Vienna, p 93-104

Nier AO, Schlutter DJ (1990) Helium and neon in stratospheric particles. Meteoritics 25:263-267

Nier AO, Schlutter DJ (1992) Extraction of helium from individual interplanetary dust particles by step-heating. Meteoritics 27:166-173

Nier AO, Schlutter DJ (1993) The thermal history of interplanetary dust particles collected in earth's stratosphere. Meteoritics 28:675-681

Nier AO, Schlutter DJ, Brownlee DE (1990) Helium and neon isotopes in deep Pacific Ocean sediments. Geochim Cosmochim Acta 54:173-182

Nightingale PD, Malin G, Law CS, Watson AJ, Liss PS, Liddicoat MI, Boutin J, Upstill-Goddard RC (2000a) *In situ* evaluation of air-sea gas exchange parameterizations using novel conservative and volatile tracers. Global Biogeochem Cycl 14:373-387

Nightingale PD, Liss PS, Schlosser P (2000b) Measurement of air-sea gas transfer during an open ocean algal bloom. Geophys Res Lett 27:2117-2120

Östlund HG (1982) The residence time of the freshwater component in the Arctic Ocean. J Geophys Res 87:2035-2043

Östlund HG, Craig H, Broecker WS, Spencer D (1987) GEOSECS Atlantic, Pacific, and Indian Ocean Expeditions. Vol 7, Shore-based Data and Graphics. National Science Foundation, Washington DC

Ozima M, Takayanagi M, Zashu S, Amari S (1984) High ^{3}He/^{4}He ratios in ocean sediments. Nature 311:449-451

Patterson DB, Farley KA (1998) Extraterrestrial ^{3}He in seafloor sediments: Evidence for correlated 100kyr periodicity in the accretion rate of interplanetary dust, orbital parameters, and Quarternary climate. Geochim Cosmochim Acta 62:3669-3682

Patterson DB, Farley KA, Schmitz B (1998) Preservation of extraterrestrial ^{3}He in 480-Ma-old marine limestones. Earth Planet Sci Lett 163:315-325

Robbins PE, Jenkins WJ (1998) Observations of temporal changes of tritium-He-3 age in the eastern North Atlantic thermocline: Evidence for changes in ventilation? J Mar Res 56:1125-1161

Robbins PE, Price JF, Owens WB, Jenkins WJ (2000) The importance of lateral diffusion for the ventilation of the lower thermocline in the subtropical North Atlantic. J Phys Oceanogr 30:67-89

Roether W, Fuchs G (1988) Water mass transport and ventilation in the Northeast Atlantic derived from tracer data. Philos Trans R Soc London, Ser. A 325:63-69

Roether W, Kromer B (1978) Field determination of air-sea gas-exchange by continuous measurement of Rn-222. Pure Appl Geophysics 116:476-485

Roether W, Münnich KO, Östlund HG (1970) Tritium profile at the North Pacific (1969) Geosecs Intercallibration Station. J Geophys Res 75:7672-7675

Roether W, Schlosser P, Kuntz R, Weiss W (1992) Transient-tracer studies of the thermohaline circulation of the Mediterranean. *In* Winds and Currents of the Mediterranean Basin: Reports in Metereology and Oceanography 41, Vol. 2. H Charnock (ed) p 291-317

Roether W, Roussenov VM, Well R (1994) A tracer study of the thermohaline circulation of the eastern Mediterranean. *In* Ocean processes in climate dynamics: Global and Mediterranean examples. Malanotte-Rizzoli P, Robbinson AR (eds) Kluwer Academic, Norwell, Massachusetts, p 371-394

Roether W, Manca BB, Klein B, Bregant D, Georgopoulos D, Beitzel V, Kovacevic V, Luchetta A (1996) Recent changes in eastern Mediterranean deep waters. Science 271:333-335

Roether W, Well R, Putzka A, Rüth C (1998) Component separation of oceanic helium. J Geophys Res 103(C12):27931-27946

Rüth C, Well R, Roether W (2000) Primordial He-3 in South Atlantic deep waters from sources on the Mid-Atlantic Ridge. Deep-Sea Res Part I 147:1059-1075

Schlosser P (1986) Helium: a new tracer in Antarctic oceanography. Nature 321:233-235

Schlosser P (1992) Tritium/^{3}He dating of waters in natural systems. *In* Isotopes of noble gases as tracers in environmental studies, Intl Atom Energy Agency, Vienna, p 123-145

Schlosser P, Bayer R, Foldvik A, Gammelsrod T, Rohardt G, Münnich KO (1990) O-18 and helium as tracers of ice shelf water and water/ice interaction in the Weddel Sea. J Geophys Res 95(C3):3253-3263

Schlosser P, Bönisch G, Rhein M, Bayer R (1991) Reduction of deep water formation in the Greenland Sea during the 1980s - Evidence from tracer data. Science 251:1054-1056

Schlosser P, Bönisch G, Kromer B, Loosli HH, Buehler R, Bayer R, Bonani G, Koltermann KP (1995) Mid-1980s distribution of tritium, ^{3}He, ^{14}C and ^{39}Ar in the Greenland/Norwegian Seas and the Nansen Basin of the Arctic Ocean. Prog Oceanogr 35:1-28

Schlosser P, Bullister JL, Fine R, Jenkins WJ, Key R, Lupton J, Roether W, Smethie WM (2001) Transformation and age of water masses. *In* Ocean circulation and climate. Academic Press, p 431-452

Smethie WM, Takahashi T, Chipman DW, Ledwell JR (1985) Gas exchange and CO_2 flux in the tropical Atlantic Ocean determined from ^{222}Rn and pCO_2. J Geophys Res 90:7005-7022

Solomon S, Burkholder JB, Ravishankara AR, Garcia RR (1994) Ozone depletion and global warming potential of CF3I. J Geophys Res 99(D10):20929-20935

Suess HE, Wänke H (1965) On the possibility of a helium flux through the ocean floor. Prog Oceanogr 3:347-353

Takayanagi M, Ozima M (1987) Temporal variation of ^{3}He/^{4}He ratio recorded in deep-sea sediment cores. J Geophys Res 92:12531-12538

Thiele G, Roether W, Schlosser P, Kuntz R, Siedler G, Stramma L (1986) Baroclinic flow and transient tracer fields in the Canary Cape Verde Basin. J Phys Oceanogr 16:814-826

Tilles D (1966) Atmospheric noble gases from extraterrestrial dust. Science 151:1015-1018

Tilles D (1967) Extraterrestrial excess ^{36}Ar and ^{38}Ar concentrations as possible accumulation-rate indicators for sea sediments. Icarus 7:94-100

Top Z, Clarke WB (1983) Helium, neon and tritium in the Black Sea. J Mar Res 41:1-17

Torgersen T (1989) Terrestrial helium degassing fluxes and the atmospheric helium budget: Implications with respect to the degassing processes of continental crust. Chem Geol 79:1-14

Unterweger MP, Coursey BM, Schima FJ, Mann WB (1980) Preparation and calibration of the 1978 National Bureau of Standards tritiated-water standards. Intl J Appl Rad Isotopes 31:611-614

von Faltings V, Harteck P (1950) Der Tritiumgehalt der Atmosphäre. Z Naturforsch 5a:438-439

Wanninkhof R (1992) Relationship between wind-speed and gas exchange over the ocean. J Geophys Res 97 (C5):7373-7382

Wanninkhof R, Asher W, Weppernig R, Chen H, Schlosser P, Langdon C, Sambrotto R (1993) Gas transfer experiment on Georges Bank using 2 volatile deliberate tracers. J Geophys Res 98(C11):20237-20248

Wanninkhof R, Hitchcock G, Wiseman WJ, Vargo G, Ortner PB, Asher W, Ho DT, Schlosser P, Dickson ML, Masserini R, Fanning K, Zhang JZ (1997) Gas exchange, dispersion, and biological productivity on the west Florida shelf: Results from a Lagrangian tracer study. Geophys Res Lett 24:1767-1770

Watson AJ, Upstill-Goddard RC, Liss P S (1991) Air-sea gas exchange in rough and stormy seas measured by a dual tracer technique. Nature 349:145-147

Weiss RF (1971) Solubility of helium and neon in water and seawater. J Chem Eng Data 16:235-241

Weiss W, Roether W (1980) The rates of tritium input to the world oceans. Earth Planet Sci Lett 49: 435-446

Weiss W, Bullacher W, Roether W (1979) Evidence of pulsed discharge of tritium from nuclear energy installations in Central European precipitation. *In* Behavior of Tritium in the Environment (Proc Symp, San Francisco), Intl Atom Energy Agency, Vienna, p 17-30

Well R, Lupton J, Roether W (2001) Crustal helium in deep Pacific waters. J Geophys Res 106(C7): 14165-14177

Weppernig R, Schlosser P, Khatiwala S, Fairbanks RG (1996) Isotope data from Ice Station Weddell: implications for deep water formation in the western Weddell Sea. J Geophys Res :25,723-25,739

Winckler G, Suess E, Wallmann K, De Lange GJ, Westbrook GK, Bayer R (1997) Excess helium and argon of radiogenic origin in Mediterranean brine basins. Earth Planet Sci Lett 151:225-233

Winckler G, Kipfer R, Aeschbach-Hertig W, Botz R, Schmidt M, Schuler S, Bayer R (2000) Sub-seafloor boiling of Red Sea Brines: New indication from noble gas data. Geochim Cosmochim Acta 64:1567-1575

Winckler G, Aeschbach-Hertig W, Kipfer R, Botz R, Rübel AP, Bayer R, Stoffers P (2001a) Constraints on origin and evolution of Red Sea brines from helium and argon isotopes. Earth Planet Sci Lett 184: 671-683

Winckler G, Anderson RF, Schlosser P, Stute M (2001b) Constant export productivity in the Equatorial Pacific through the Mid-Pleistocene Climate Transition - New evidence from an extraterrestrial ^{3}He record. EOS Trans Am Geophys Union, Fall Mtg Suppl 8:F636